AN ABSTRACT OF THE THESIS OF

KEITH GOODIN CROUCH for the degree DOCTOR OF PHILOSOPHY
(Name) (Degree)

in PHYSICS presented on June 12, 1974
(Major Department) (Date)

Title: SURFACE EFFECTS IN PHOTOEMISSION FROM POTASSIUM

Redacted for privacy

Abstract approved: _____
Dr. James J. Brady

The photoelectric yield vs wavelength was measured for thick potassium deposits, and for potassium with various measured coverages of sulfur of the order of a monolayer. The samples were deposited and maintained at liquid nitrogen temperatures. The vacuum system maintained the pressure in the mid-10^{-11} Torr range after deposition. The deposition masses were measured by direct deposition onto a quartz crystal, which was the active element in a quartz oscillator microbalance.

A time dependent decrease of the yield for pure potassium was observed, and appears to be due to a decrease in the surface roughness, which decouples the light from the surface plasmon excitation.

A double threshold was observed for several of the pure potassium depositions, the higher threshold at 2.40 eV and the lower at 2.00 eV. Explanations offered are the presence of surface states or

the presence of two crystallite orientations in the deposit.

The sulfur introduced what is interpreted as a second peak in the yield vs wavelength curve, which appears to be due to excitation of electrons from the sulfur valence band. The change in work function vs sulfur thickness curve was fitted using Lang and Kohn's theory (Physical Review B 3:1215-1222. 1971).

The results emphasize the importance of surface configuration variables in photoemission from the alkali metals, and indicate the need for a simultaneous determination of such variables along with the photoemission studies, in order to determine which variables are significant.

Surface Effects in Photoemission from Potassium

by

Keith Goodin Crouch

A THESIS

submitted to

Oregon State University

in partial fulfillment of
the requirements for the
degree of

Doctor of Philosophy

June 1975

APPROVED:

Redacted for privacy

Professor of Physics
in charge of major

Redacted for privacy

Chairman of Department of Physics

Redacted for privacy

Dean of Graduate School

Date thesis is presented June 12, 1974

Typed by Clover Redfern for Keith Goodin Crouch

ACKNOWLEDGMENTS

Those to whom special thanks are appropriate are: Dr. James J. Brady, for his helpful suggestions and general support throughout the project; Rodney Whitefield, for the construction of most of the apparatus, for providing detailed directions on its use, when necessary, and for many helpful discussions in all areas of the work; Allen Wasserman, for stimulating and helpful discussions of some of the theoretical aspects; and C.G. Sahasrabuddhe, for help in obtaining the transmission coefficients of the light filters and window.

TABLE OF CONTENTS

LIST OF FIGURES

LIST OF TABLES

SURFACE EFFECTS IN PHOTOEMISSION FROM POTASSIUM

I. INTRODUCTION

The work that this thesis is concerned with had two major objectives. The first was to determine the photoelectric work function of potassium under extremely good vacuum conditions. The second was to determine the changes in the photoelectric properties of a potassium surface contaminated with small but measurable amounts of pure sulfur.

Previous workers have reported values of the work function of potassium which differed from one another by considerable amounts. At least some of this discrepancy is most likely the results of poor vacuum conditions, since the potassium surface under these conditions would be contaminated by the residual gases.

Olpin (41) reported considerable changes in the photoelectric properties of the alkali metals when exposed to traces of sulfur vapor. He made no attempt to determine the amount of sulfur which produced the changes in the photoelectric response. By studying the response of pure potassium, and then the effects of known amounts of a contaminating species which produces a large change in the response, one can get an idea of the maximum sensitivity to contamination to be expected of the photoelectric response.

Photoemission from pure alkali metals has been studied experimentally several times (3, 4, 9, 34, 38, 47, 50), partially due to their simple electronic energy states. There has been a notable lack of agreement between different investigators, and a problem with reproducibility of results of the same investigator. Part of this variation is due to the high reactivity of the alkali metals and has been largely eliminated by relatively recent improvement in vacuum techniques. However, there are still some uncontrolled variables leading to non-reproducibility of certain aspects of the photoemission. This problem appears to be associated mainly with the sensitivity of the photoemission to the surface configuration, its roughness, variation of the lattice constant near the surface, reconstruction of the surface region, defects, and contamination, all of which have only recently yielded somewhat to quantitative determination.

Of the above surface configuration variables, only the surface roughness has been included in a general theory of photoemission (13), through its role in the light-surface plasmon coupling and light scattering problem (1, 11, 23, 24). However, no first-principles theory of photoemission from simple metals has been advanced that fits the experimental data well from the threshold through the bulk plasmon frequency. The Fowler theory of yield vs wavelength fits reasonably well near the threshold, but it needs two adjustable parameters to fit a range of materials. Calculations of the surface

photoelectric effect (12, 17, 33, 36, 37) from perturbation theory, assuming a free-electron gas as starting point, may give a peak at the surface plasmon frequency, but the shape is wrong, and the only attempt at a partially self-consistent calculation (17) did not have the peak properly located.

Certain aspects of the theory of photoemission have been covered, such as the variation of work function with thickness of contamination. Nearly all of this work has been done for a metallic substrate with a metallic (usually alkali metal) adsorbate (15, 19, 22, 40). The theory of Lang and Kohn (27, 28) on metallic work functions is directly applicable to the present investigation, since it provides a formulation for alkali metal substrates with an arbitrary adsorbate, specified by its perturbation of the metallic potential. In principle, there are no adjustable parameters in this theory, but in practice, a lack of information as to the location of the adsorbate with respect to the metal surface and the effects on the adsorbate of the interaction between the metal and the adsorbate lead to two adjustable parameters.

This investigation, which is a sequel to a similar one done on sodium (49), was initiated primarily for two reasons. First, Whitefield worked out a method for decreasing the contamination of the freshly deposited potassium samples, by keeping the deposition sources in a separate vacuum chamber from the one in which the depositions took place. The two chambers had a straight-through

valve connecting them, so that immediately after a deposition, the valve could be shut, eliminating to a large extent the possibility of contamination by out-gassing of the hot deposition sources. This technique resulted in a significantly higher work function for sodium than reported by other investigators, which led Whitefield to suggest that most workers may have used contaminated samples (53). And by analogy, we thought that data for potassium may have been influenced by contamination, also, which Whitefield's technique would help to eliminate. The results of this experiment suggest other possible causes of this discrepancy.

Second, it was thought that some light might be shed on the variation of work function with sulfur adsorbate thickness. For sodium as a substrate, the work function decreased from its initially high value to a minimum at about two monolayers of sulfur, and then increased with larger thicknesses of sulfur. The explanation offered for the initial decrease in the work function was based on the assumption that the first layer of deposited sulfur atoms would reside in sites below the sodium surface. If the initial sulfur layer went on the top of the surface for potassium, it was expected that the work function would then increase monotonically. The results of this investigation, with the help of the theory of Lang and Kohn (27), do appear to explain this variation.

The experimental work involved was the determination of the photoelectric yield per incident photon vs wavelength of monochromatic light, for pure potassium and for potassium with various measured amounts of sulfur deposited as contamination on the potassium substrate. The deposits were made on the chromium-coated gold electrodes of an optically flat quartz crystal, which was the active element of a quartz oscillator microbalance. The quartz crystal was maintained at liquid nitrogen temperatures (77°K).

The pure potassium was obtained in glass ampoules and transferred to an evaporation well in a bell-jar vacuum system. The evaporation well was then removed from the bell-jar system and connected to the lower vacuum system, which was isolated from the upper system by a straight-through valve. The upper system contained the quartz crystal upon which the deposits were made. With this arrangement, contamination of the fresh deposit by out-gassing from the hot evaporation sources could be largely eliminated by closing the straight-through valve immediately after deposition. Pressures in the mid-10^{-11} Torr range were achieved and maintained in about a half-hour after completion of a deposit.

The incident light intensity for the photocurrent measurements was measured with a Reeder thermopile. The photocurrent was measured with a Cary 31 vibrating-reed electrometer.

The main features of the results on pure potassium are a large peak in the yield at the surface plasmon frequency, the amplitude of which is time-dependent, and a double threshold for most of the samples, with work functions of about 2.4 eV and 2.0 eV. For the sulfur contaminated samples, a second peak at a light energy of 3.5 eV appears at 1 to 2 monolayers of sulfur, the surface plasmon-associated peak migrates to a lower energy, the work function decreases from 2.4 eV to about 2.0 eV at about 2 monolayers, and the amplitude of the yield first increases out to about 1.5 monolayers, and then decreases as more sulfur is added. Representative data are shown in the Appendix, including a family of yield vs wavelength curves for various times after deposition of the pure potassium, and a series of yield vs wavelength curves for various sulfur coverages. Also included is a table of work functions obtained for pure potassium. Other data are included at the appropriate places in the body of the report.

II. PREPARATION AND MAINTENANCE OF SAMPLES

A. Preliminary

The potassium used was 99.95% pure, as obtained from M.S.A. Research Corporation, Evans City, Pennsylvania. It was sealed under vacuum in glass ampoules during shipment, but had been processed under argon by the vendor. An analysis of the impurities is given in Table 1.

In order to carry out an experiment with the potassium, it was necessary to transfer it from the glass ampoules to the potassium evaporation well, which was then attached to the lower vacuum system. See Figures 1, 2 and 3 for schematics of the vacuum systems. This transfer was carried out in a separate bell-jar vacuum system (Figure 3), which was roughed out with a mechanical pump to 40 microns followed by further roughing with a cryopump containing molecular sieve material cooled to the boiling point of liquid nitrogen. This system also contains a titanium sublimation pump which is used to help start the 20 liter per second Vacion and 25 liter per second D-I pumps, one of each. During this initial pumpdown, the evaporation well was located near the titanium sublimation pump filaments, and was thus being heated and pumped out simultaneously. When the pressure got down at least to the low 10^{-6} Torr range, the glass ampoule containing the potassium was heated using a tungsten filament

Table 1. Vendor's analysis of potassium impurities.

MSA RESEARCH CORPORATION
Evans City, Pennsylvania 16033

MSA RESEARCH CORPORATION ANALYTICAL REPORT

Type of Material Potassium Lot No. ST7-857-1

Grade of Material High Purity Container No. _____

Element	ppm	Element	ppm	Element	ppm
Fe	-5	Cr	-5	Sr	-1
B	-10	Si	12	Ba	-3
Co	-5	Ti	-5	Ca	1
Mn	-1	Ni	-5	Li	
Al	-2	Mo	-3	Na	4
Mg	-2	V	-1	K	Balance
Sn	-5	Be	-1	Rb	
Cu	2	Ag	-1	Cs	
Pb	-5	Zr	-10	O_2	
				C	

Remarks: The prefix - designates less than.

Metallic impurity levels reflect analysis of the chloride form of the metal.

Reference: Emission Spec Analysis - 13034-13032
12977-12987

NUMEC Plate No. 11582

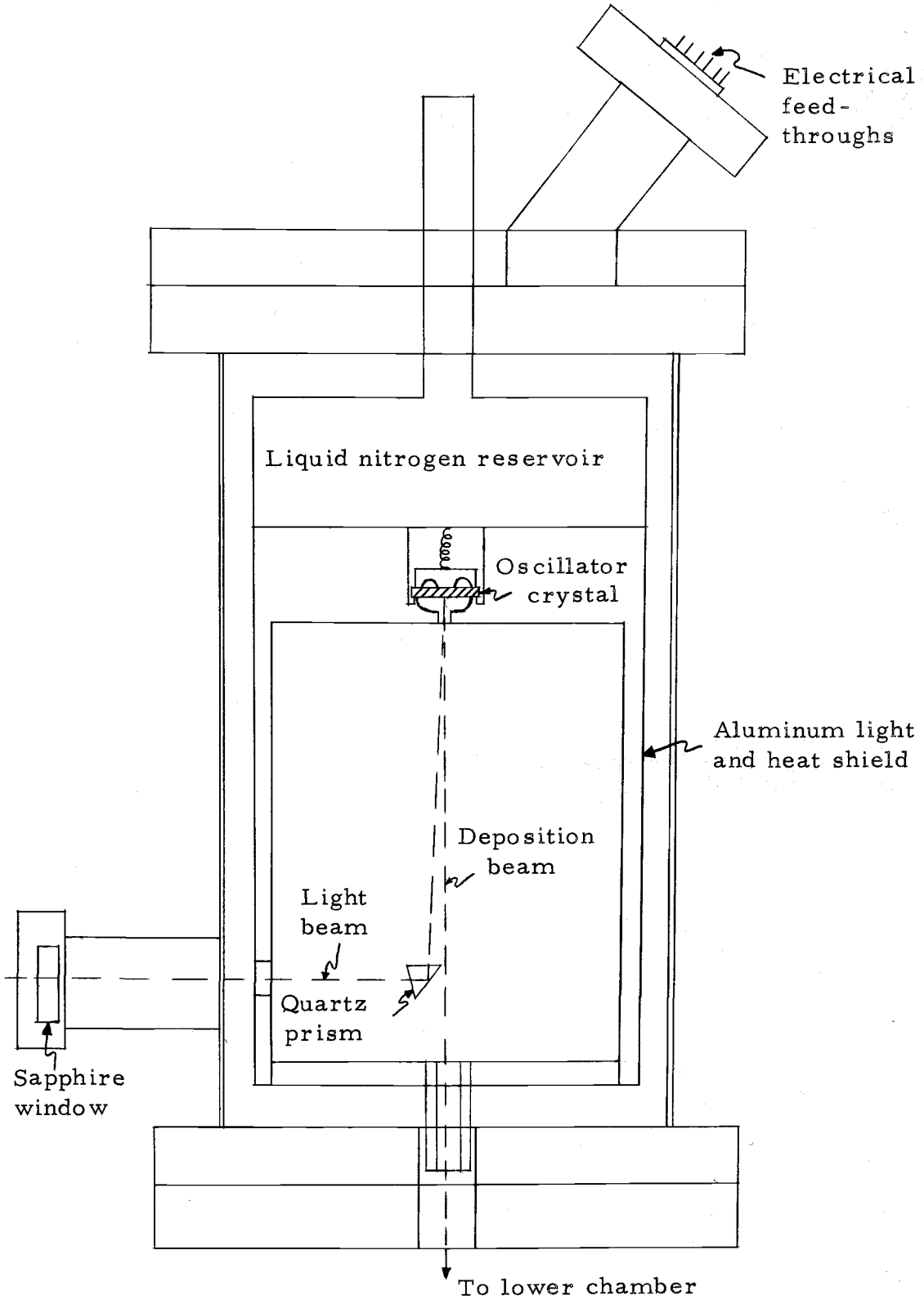

Figure 1. Schematic diagram of upper chamber of vacuum system. Not to scale.

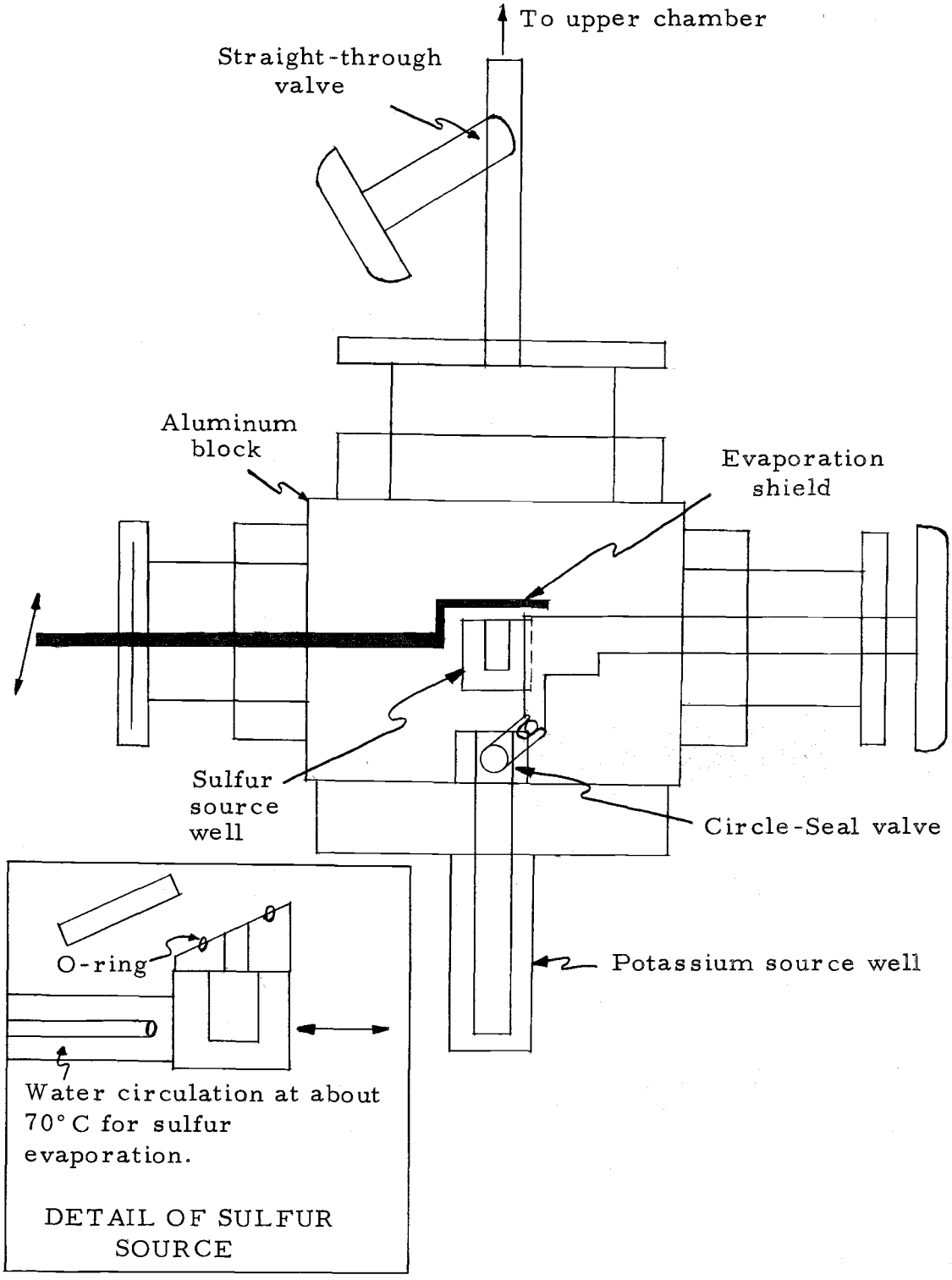

Figure 2. Schematic diagram of lower chamber of vacuum system. Not to scale. Pumps and pumping ports are not shown.

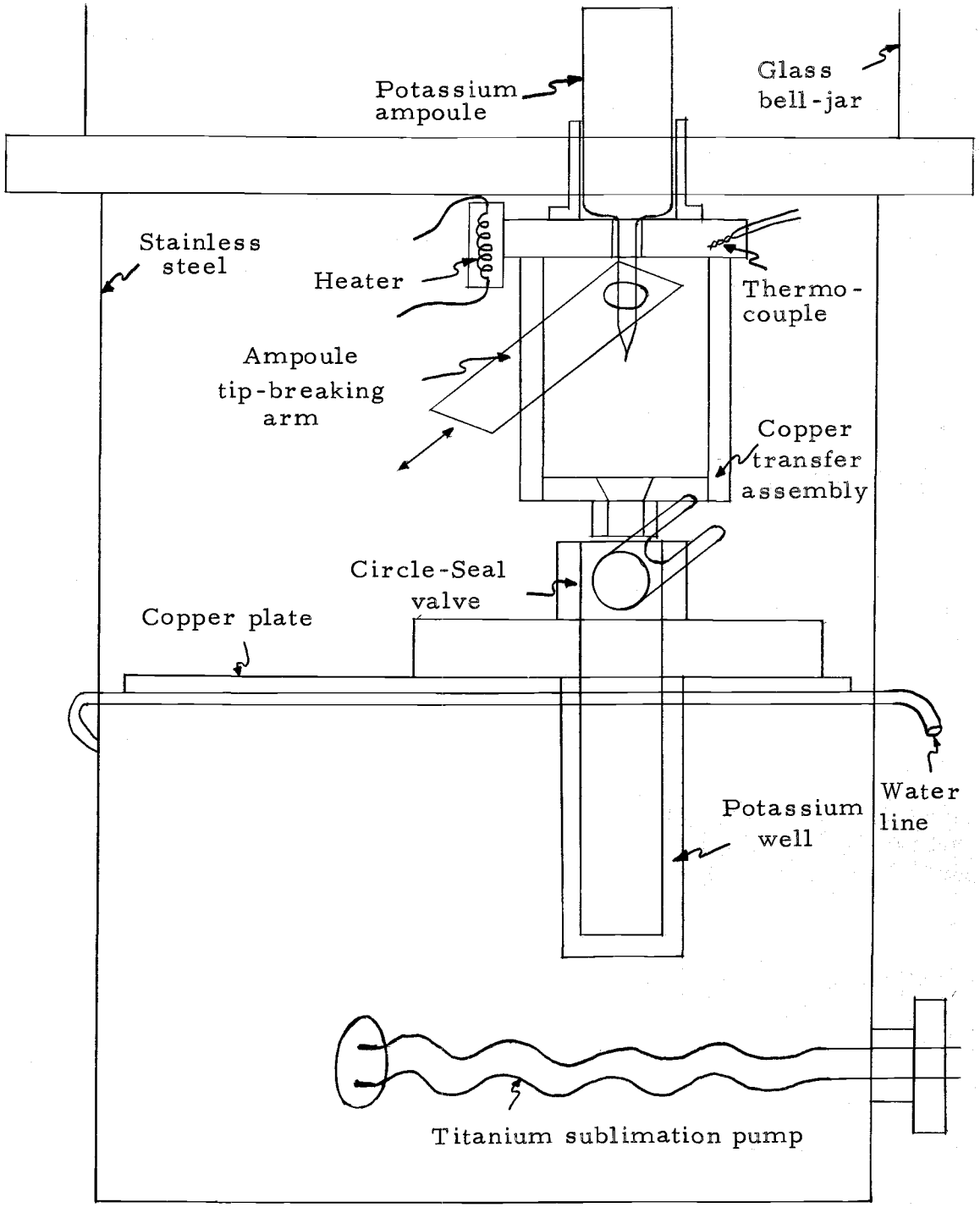

Figure 3. Schematic diagram of the bell-jar vacuum system, completely independent of the upper and lower systems, in which transfer of the potassium from the ampoules to the evaporation well was made. Only the main features are shown. The Circle-Seal valve could be actuated by a linear motion feed-through, not shown.

attached to the side of the transfer assembly (Figure 3). When the potassium melted, indicated by its running down into the tip of the glass ampoule, this tip was broken off, and the remainder of the potassium ran down through the funnel into the evaporation well. There was a large pressure increase when the ampoule was broken, which probably indicates residual argon from the processing. The surface of the potassium inside the glass ampoule always looked shiny, indicating the absence of any significant amount of reactive contaminants.

After the transfer, the evaporation well was closed and allowed to cool to room temperature. The bell jar system was then let up to atmospheric pressure by admitting prepurified nitrogen to the system, so that any leaks in the evaporation well would not cause oxidation of the potassium surface. The evaporation well had a Circle Seal valve, which contains three rubber O-rings. During one transfer attempt, this valve leaked sufficiently that a layer of oxide formed on the potassium and prevented its evaporation. This failure may have been due to deterioration of the rubber during heating. Subsequently, the O-rings were replaced at every opportunity and heating of the evaporation well was kept to the minimum possible.

Previous to the transfer, the evaporation well was cleaned thoroughly. First, it was given a warm detergent wash using a bottle brush, and rinsing in hot water. Then, water freshly distilled in this

laboratory was used to rinse it further. The resistivity of this water was monitored during the multiple rinsings, and when the discarded water had the same resistivity as the fresh water, preliminary rinsing was considered adequate. The distilled water from the building supply had a lower resistivity than the water used, by a factor of at least four, possibly due to the dissolution of atmospheric carbon dioxide in it. After this initial rinse a final rinse was made, in which the water was brought to a boil in the well before being discarded. The well was then baked for several hours at a temperature of about 200° C to get rid of any residual water, and placed in the bell jar ready for the transfer. The transfer assembly itself was also given a detergent wash, tap water rinse, and then a bath in dilute nitric acid, until a shiny copper surface appeared. It was then rinsed in distilled water, dried by baking at about 200° C, and then assembled and placed in the bell jar system ready for the transfer.

The sulfur used was 99.999+% spectrographically pure, obtained from the American Smelting and Refining Company, South Plainfield, New Jersey. A small amount of it was poured onto a piece of filter paper, and from there funneled into the sulfur evaporation well. An acetone and a distilled water rinse seemed to be adequate cleaning for this well. Following this, it was heated at about 200° C for two to three hours to get rid of any residual water, and then filled with sulfur when cool.

B. Vacuum Systems

In order to keep a freshly deposited layer of potassium free from contamination, it is necessary that the partial pressure of reactive gases in the vacuum be kept very low. Towards this end, the evaporation sources were kept in a separate vacuum system from the deposited sample. There was a tube with a valve in it connecting the chambers (Figure 2). As soon as an evaporation was completed this valve was closed, so that a minimum of contaminants from the hot well regions could get to the fresh surface. This valve could be completely closed in 10 to 15 seconds after completion of the deposition, and the pressure in the sample chamber dropped from 2×10^{-9} Torr during evaporation to about 10^{-10} Torr in five minutes, and nearly to the base pressure of about 5×10^{-11} Torr in a half-hour after the deposition. A typical potassium deposition takes 30 minutes, giving a deposit 2110 Å thick.

In order to get an idea of the possible contamination effects on the fresh surface, the time required for the impact of a number of residual gas atoms equal to the number of atoms in a monolayer of potassium is calculated. The rate of collision per unit area of the residual gas atoms of mass m, temperature T and pressure p is given by

$$\frac{dn}{dt} = (2\pi mkT)^{-1/2} p \ .$$

See reference (32). For hydrogen molecules at 295°K and a pressure of 5×10^{-11} Torr, this gives 7.20×10^{10} molecules-cm^{-2}-sec^{-1} striking the surface. There are 5.76×10^{15} potassium atoms per cm^2 in a monolayer of potassium, giving a monolayer impact time of about 8×10^4 sec, or 22.2 hours. This is a lower limit on the impact time, since other gases have a greater mass than hydrogen. An experimental run on pure potassium took one week, approximately, giving time for the impact of up to 7.6 monolayers of the residual gases. However, no effects expected from contamination, such as a shift in the work function or the location of the peak in the yield, were observed over this period (see the Appendix), meaning that the sticking coefficient for the residual gases is much less than one, so that most of these gases are not reactive with the potassium.

The upper vacuum chamber, in which the samples were deposited and maintained, was constructed of stainless steel, with OFHC copper gaskets in the sealing flanges and a sapphire window to admit light. There are two 8 liter/second sputter-ion pumps connected to this chamber, only one of which was needed to maintain the low pressures after the initial pump-down stages. There is also a titanium sublimation pump connected to the chamber, and a nude Bayard-Alpert ionization gauge is located in a tube connected to the main vacuum chamber, so that one end of the gauge is in this chamber. The liquid nitrogen well, used to cool the samples, has its

walls inside this chamber, providing significant cryopumping.

Initially, a bakeout of the upper chamber preparatory to pump-down was made at 400° C, but this caused cracking of a welded joint, and failure of an electrical feed-through, so the bakeout temperature was reduced to 220° C, for about 15 hours. During the bakeout, which included all parts of the upper system, the evolved gases were pumped with a cryopump containing molecular sieve material maintained at liquid nitrogen temperatures. After bakeout, with the cryopump valved off, it typically took three to four days for the sputter-ion pump to reduce the pressure to the 10^{-11} Torr range, so that experimentation could begin.

The lower system consisted of a machined aluminum block, to which was connected the sulfur and potassium wells, an 8 liter/second sputter-ion pump, and a Varian Associates partial pressure gauge, model number 974-0036. The connecting tubing was stainless steel, with OFHC copper gaskets in the flanges. The greatest portion of this system was baked out with heater tape and heat lamps at over 100° C for 12 hours while connected to a cryopump containing molecular sieve material maintained at liquid nitrogen temperatures. The base pressure of this system was in the high 10^{-9} Torr region.

C. Microbalance and Depositions

A quartz crystal microbalance was used to determine the mass of the depositions. The crystal was 1/2 inch in diameter, with a nominal 5 MHz fundamental. The electrodes were chromium-coated gold in the keyhole configuration with a circular sensitive area 1/4 inch in diameter. Depositions were made on a circular region 0.159 inch in diameter centered on the active area of one of the electrodes.

The crystal was in an aluminum holder that was in good thermal contact with a reservoir containing liquid nitrogen. In the holder, the crystal rested on a circular ledge with four sections cut out, so that stainless steel electrodes could be clipped onto the crystal electrodes. This ledge contacted the crystal only near its edge, in an inactive portion of the crystal. A cup-shaped piece, also with four sections cut out of its lip, was placed on top of the crystal, contacting it again only near its edge. The cup-shaped piece was held in place with a spring, which pushed against the liquid nitrogen reservoir. The crystal was AT-cut, at an angle of $39°44' \pm 1'$, in order to give a zero temperature coefficient of frequency at 78.2°K, near the boiling point of liquid nitrogen. The crystal was operated at about 15 MHz in a third overtone, and at this frequency, a change of temperature of one degree Kelvin from 78.2°K will change the resonant frequency by 2/3 Hz (45).

The circuit used to excite the quartz crystal and to monitor its resonant frequency has been discussed (14). It consists basically of an oscillator section to drive the crystal, and a buffer and amplifier section to provide power for driving a frequency counter. It was designed for stability, which will be discussed later in this section.

In order to relate the observed frequency changes Δf to the mass added during deposition Δm, the following relationship is used:

$$N \frac{\Delta f}{f} = -K \frac{\Delta m}{m} ,$$

where f is the resonant frequency (assumed constant during deposition), m is the resonating mass of the crystal plate, N is the harmonic at which the crystal is oscillating, and K is a constant, usually expected to be close to one for uniform deposits covering the whole electrode area (39, 46, 49). Clamping technique and asymmetries due to surface curvature of the crystal may also cause K to deviate from one (46, 52). Whitefield (51) determined K for a crystal essentially identical to the one used in this investigation under essentially identical conditions and found it to be 0.90 ± 0.05. One then uses the relationships $c = ft = 166.8 \times 10^3$ Hz-cm, and $m = DAt$, where t is the thickness of the crystal, D is its density (2.648 g/cm^3), and A is the deposition area (0.1233 cm^2), to get

$$\frac{\Delta m}{\Delta f} = -NDAc/Kf^2 .$$

For f, 1.5087×10^7 Hz is good to better than 0.1% for all determinations made here, so

$$\left|\frac{dm}{df}\right| = 7.98 \times 10^{-10} \text{ g/Hz}, \quad \text{or} \quad 6.48 \times 10^{-9} \text{ g/cm}^2\text{/Hz}$$

The deposits are probably all polycrystalline, but their detailed structure is not known, so some arbitrary, but consistent, definition of a monolayer of deposited atoms is needed, in order to relate the changes in frequency to the thickness of the deposits. The following seems to be a reasonable way to relate the known bulk property (density) to the assumed crystal structure.

We will assume that the potassium is deposited with a perfect b.c.c. structure, having a lattice constant at 77°K of 5.25×10^{-8} cm (54). There are two atoms per unit cell, and so potassium has a density of 0.895 g/cm^3. One unit cell of potassium contains

$$\frac{39 \text{ g/mole}}{6.02 \times 10^{+23} \text{ atoms/mole}} \times 2 \text{ atoms/unit cell}$$

$$= 12.96 \times 10^{-23} \text{ g/unit cell},$$

and one face of the unit cell has an area of

$$(5.25 \times 10^{-8} \text{cm})^2 = 27.55 \times 10^{-16} \text{cm}^2\text{/unit cell},$$

so there are

$$12.96 \times 10^{-23} / 2.755 \times 10^{-15} = 4.70 \times 10^{-8} \text{ g/cm}^2$$

in a deposit one unit cell thick. If one assumes that the mass in the unit cell is distributed uniformly throughout the cell, then the cell is $(2)^{1/3}$ atoms thick, so that there are

$$(4.70 \times 10^{-8} \text{g/cm}^2) / 1.26 = 3.73 \times 10^{-8} \text{g/cm}^2$$

in a monolayer of potassium, giving

$$(3.73 \times 10^{-8} \text{g/cm}^2) / (6.48 \times 10^{-9} \text{g/cm}^2/\text{Hz})$$

$$= 5.76 \text{ Hz/monolayer.}$$

One monolayer of potassium by this definition is 4.17 Å thick.

For sulfur, one assumes an orthorhombic unit cell, since that is the stable form in the temperature range of this experiment (35). This structure contains 16 S_8 molecules, giving 6.48×10^{-21} g/unit cell. A unit cell has dimensions 10.46 Å wide, 12.87 Å high, and 24.49 Å long. Assuming the 24.49 Å by 12.87 Å face lies on the deposition plane gives

$$(6.84 \times 10^{-21} \text{g/u.c.}) / (3.15 \times 10^{-14} \text{cm}^2/\text{u.c.})$$

$$= 2.17 \times 10^{-7} \text{ g/cm}^2$$

for a deposit one unit cell (u.c.) thick. To get the thickness in atoms

of the unit cell, one solves the system

$$xyz = 128, \quad x:y:z = 10.46:12.87:24.49,$$

where x, y, and z are the lengths in units of an atomic diameter of the sides of the unit cell, assumed to contain a uniform distribution of mass. This gives

$$x = 3.54, \quad y = 4.36, \quad z = 8.30,$$

so that one monolayer contains

$$(2.17 \times 10^{-7} g/cm^2)/(3.54) = 6.13 \times 10^{-8} g/cm^2,$$

giving

$$(6.13 \times 10^{-8} g/cm^2)/(6.48 \times 10^{-9} g/cm^2/Hz) = 9.49 \text{ Hz/ml},$$

one monolayer being 2.95 Å thick by this definition.

All of the potassium deposits were within one percent of 2930 Hz, 508 monolayers, or 2120 Å thick, except one which was 1554 Hz, 270 monolayers, or 1126 Å thick. The sulfur depositions ranged in thickness from about 1 to about 50 Hz, or from about 0.1 monolayers to about 5 monolayers.

For potassium deposits, the electronics systems were turned on and allowed to warm up for at least an hour, so that the drift was less than one Hz in five minutes. The potassium well was then heated up with a resistance heater with the Circle-Seal valve opened, and the

deposition flag covering the opening. When the temperature got to 200° C, as measured with an iron-constantan thermocouple in contact with the outside surface of the well, the straight-through valve was opened and the flag moved so the deposition could begin. All these deposits took 30 minutes ± 5 minutes, with the temperature of the well rising during this time to about 250° C. All these deposits appeared smooth, with no apparent diffuse reflection. When the required thickness was reached, the flag was moved to cover the well, then the straight-through valve was closed simultaneously with the Circle-Seal valve. The oscillator frequency typically fluctuated slightly (less than ± 1 Hz) during the first minute after completion of the deposition, and then settled down to its pre-deposition stability, indicating that some slight heating effects of the quartz crystal were taking place during deposition.

For sulfur depositions, more care was required to achieve the stability necessary for a reasonably precise determination of Δf. Typically, Δf was about 2 Hz for each sulfur deposition, which took about 1 minute. Stability and drift considerations lead to a maximum error of about 0.2 Hz, or 10%, in this determination. This kind of stability could only be achieved after at least two hours of warmup, with the doors and windows closed to reduce variations due to air current-induced changes in circuit parameters. Also, the frequency was recorded continuously, so that the difference in average frequency

for five minute periods before and after the deposition could be taken, to reduce the effects of random variations and the temperature induced fluctuations appearing after the deposition. Under the "best" conditions, the error in Δf could be reduced to 0.1 Hz, but it was never determined just what the critical factors were that influenced the stability at this level. Figure 4 shows a typical frequency vs time recording for a sulfur deposition.

The partial pressure gauge (PPG) was used during two potassium depositions to determine possible contaminants of the fresh deposit. The residual gas pressures were measured before heating of the well, and during heating. A comparison of these two data sets indicates that the only additional constituent appearing during heating was potassium. The primary constituents of the background gases were water vapor and nitrogen. The PPG was connected to the lower chamber of the vacuum system.

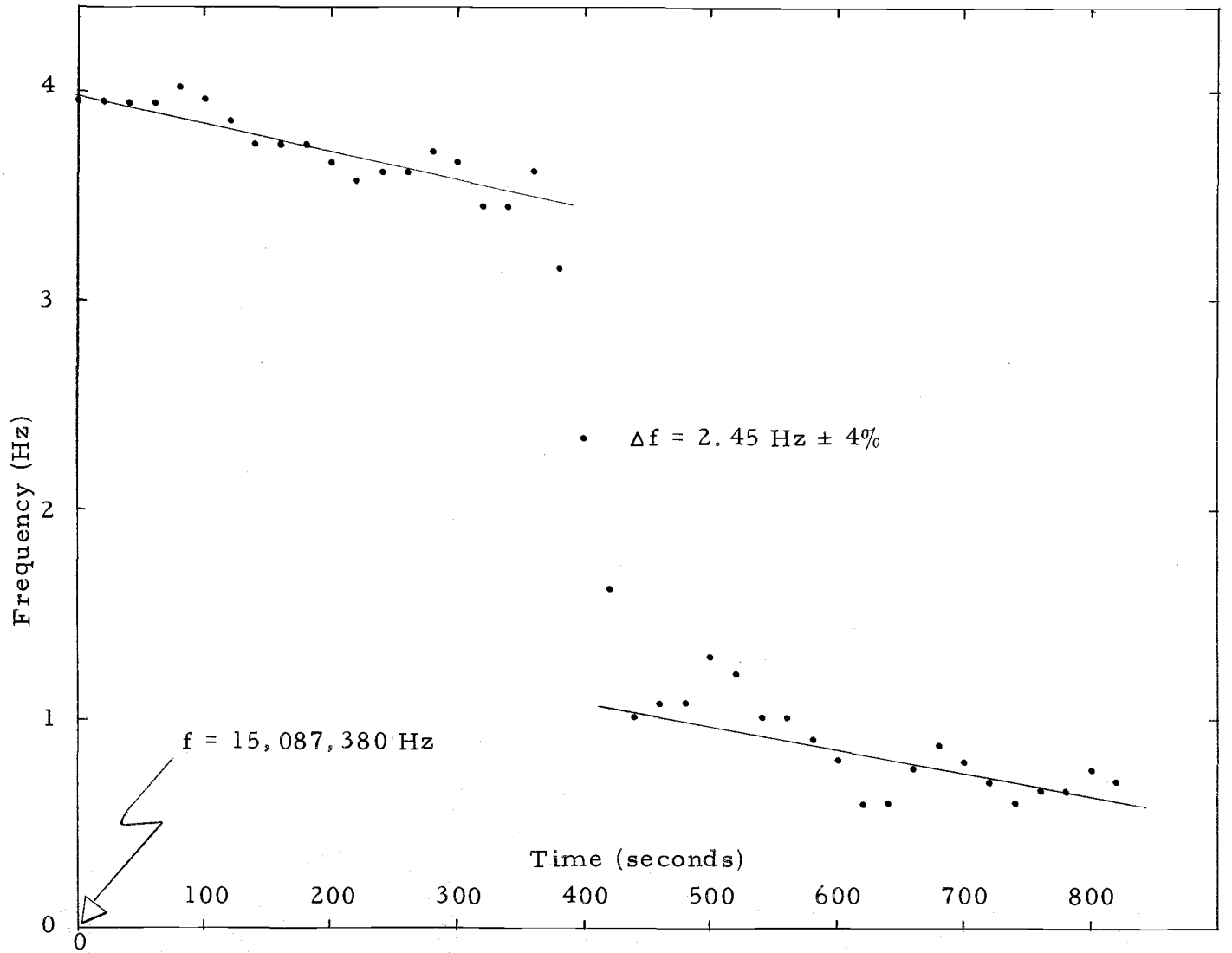

Figure 4. Typical deposition: frequency vs time.

III. DETERMINATION OF THE PHOTOELECTRIC YIELD

A. Preliminary

The yield Y is defined by $Y = N_e/N_p$, where N_p is the number of monoenergetic photons incident on the sample, and N_e is the number of electrons emitted. The quantities directly measured in this investigation were the photocurrent I, the voltage output V from a thermopile, and the wavelength of the light, L. One can show that $Y \propto I/LP$, where P is the power of the incident light. The Reeder thermopile used, which was blackened for use in the ultraviolet, has its voltage output V directly proportional to the light power P incident on the surface. Its response is essentially independent of frequency over the range involved in this experiment (30). Thus, $Y \propto I/LV$, and this proportion will be taken as an equality for experimental purposes, so that the measured yields are really relative yields, not absolute yields.

The elements in the light system are shown in Figures 5 and 6. The light source is a 400 watt quartz-iodine lamp, made by General Electric, model number Q400 T4/CL. Current for this lamp was provided as shown in Figure 5 by a voltage-regulated supply giving 115 v a. c. The current was adjusted precisely to 3.50 amperes after about a one-hour warm-up period, and remained constant to within about 0.3% throughout a run, small adjustments to the current being

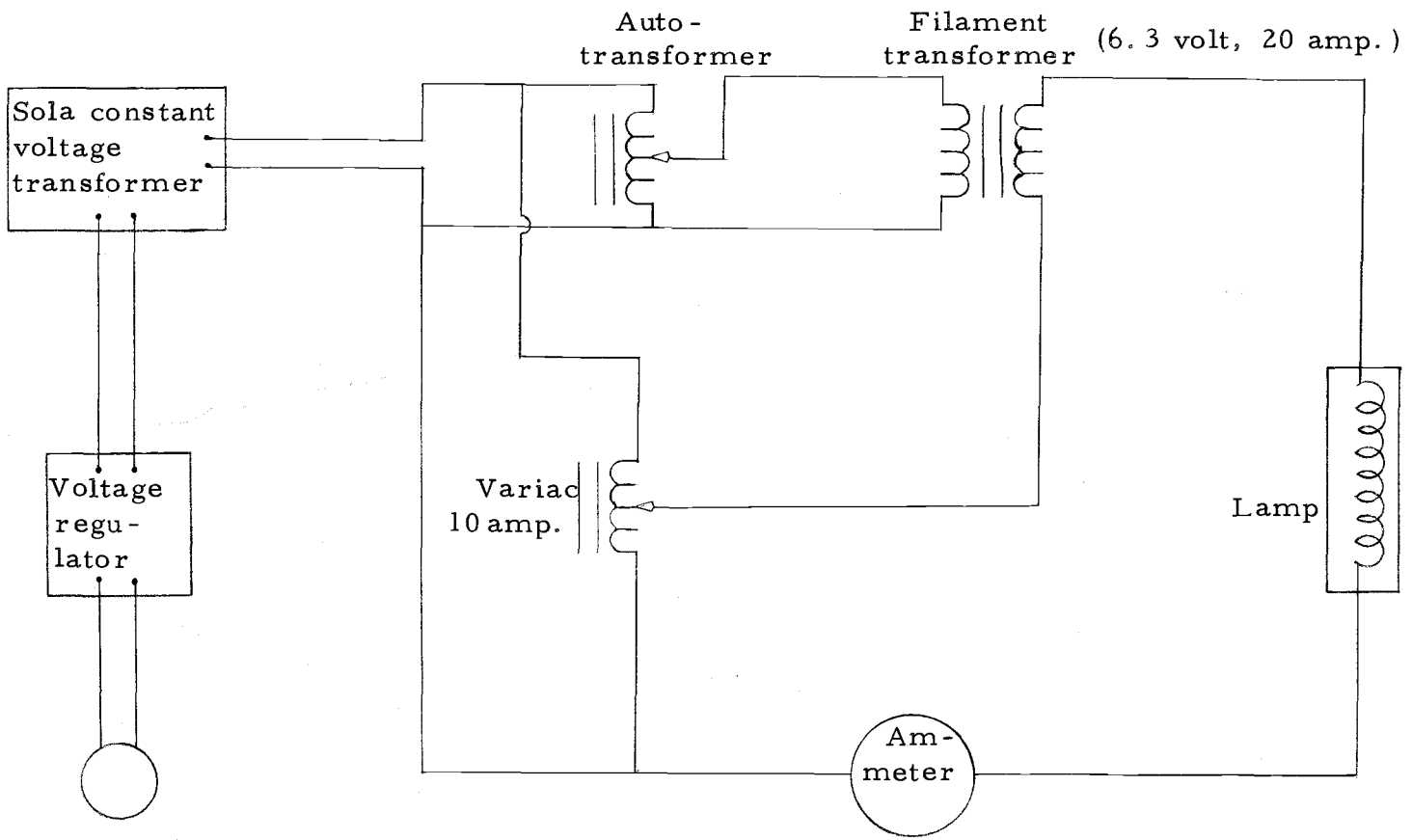

Figure 5. Lamp power supply. Variac gives rough current adjustment. Auto-transformer gives fine current adjustment.

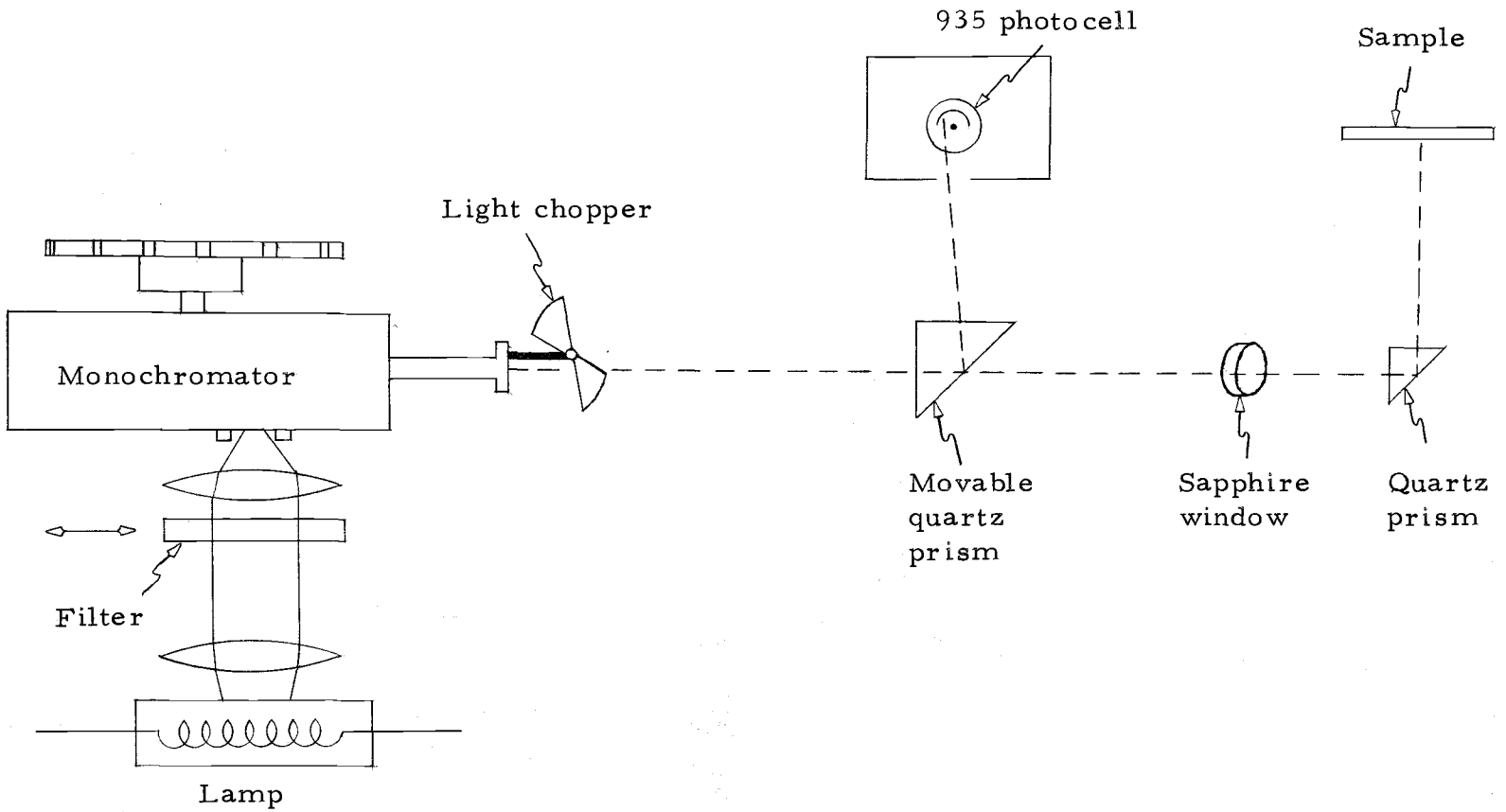

Figure 6. Light system schematic. The light travels in vacuum to the right of the sapphire window.

made periodically during the run to correct for drifts caused by any ambient temperature changes. A 0.3% change in the lamp current could typically just produce the minimum detectable change in the photocurrent.

The output of the monochromator was monitored periodically by a 935 photocell during the period of time for which data were collected. The ratio of this photocurrent at each monochromator setting to the photocurrent at the corresponding setting for the original determination was calculated, and found to vary by less than 1/2% from the average ratio for any one determination, except near the tails of the response curve of the photocell. The average ratio was found to vary by less than one percent from the initial determination over this time period. This means that there was essentially no variation in the spectral distribution of the output of the lamp and monochromator during this period, and no significant variation in their overall intensity. The intensity was taken to be constant throughout these measurements.

The monochromator used is a Bausch and Lomb 250 mm grating type instrument. In order to eliminate second order light, a Corning type CS3-72 filter was used starting from 4810 Å, and for longer wavelengths. Data were also taken up to 5060 Å with no filter, with the overlapping region used to join the filtered and unfiltered portions of the data smoothly. The transmission coefficient of this filter,

measured with a Cary 15 spectrophotometer, is shown in Figure 7.

In order to check for scattered infrared light from the monochromator, which might interfere with measurements at the shorter wavelengths, where the lamp output is comparatively low, representative data were taken with and without a CS7-54 filter, which transmits over a band from about 2400 Å to 4100 Å (1% transmission points). The transmission coefficient of this filter was determined on the Cary 15, and is shown in Figure 7. These measurements indicate that no effects of scattered light with wavelength longer than 4100 Å can be detected in the photocurrent data, down to the shortest wavelength for which data were taken, 3056 Å. The wavelength drum of the monochromator was connected to a Geneva drive, which rotates the drum through a nine degree angle every time a pulse is received, initiated from a remote switch. The position settings (p.s.) of the drum defined by this drive mechanism were calibrated by observation of eight lines of the mercury spectrum, from 3126 Å to 5791 Å. A least-squares fit to a straight line gave $L = 50.1\ (p.s.) - 200$, where L is the wavelength of the light in angstroms. This calibration was carried out twice, once near the beginning of data acquisition and once near the end, with no significant differences. Data were normally taken with the drum rotating in one direction only. A check of the validity of this procedure was made by stepping the drive back and forth through a peak in the photocurrent, with identical results for

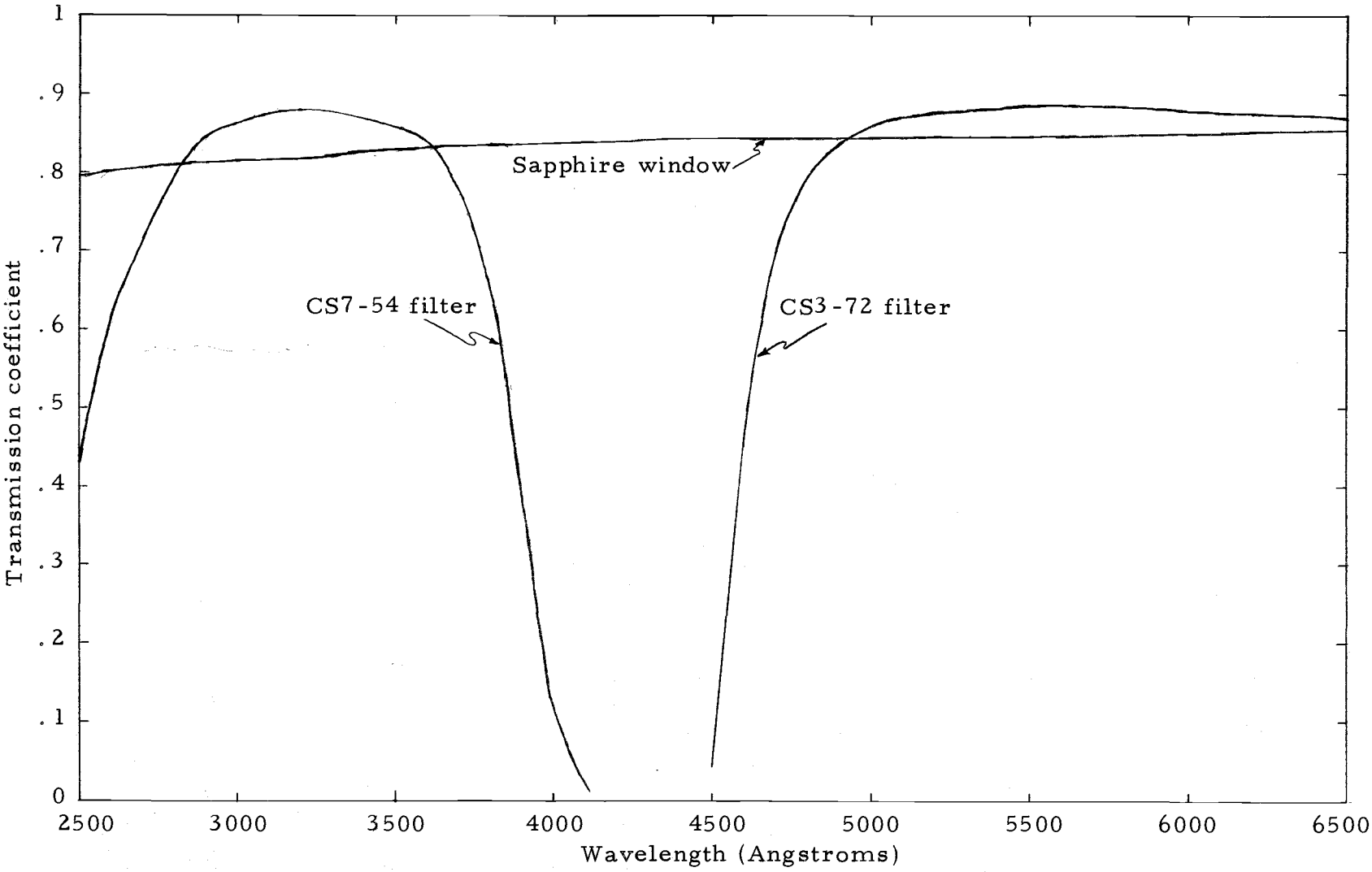

Figure 7. Transmission coefficients, determined on a Cary 15 spectrophotometer.

each direction. The bandwidth of the monochromator was determined at several wavelengths by visual observation of mercury and sodium arc lines. A value of between 45 and 50 Å was obtained, corresponding to an exit slit width of 0.4 mm. The other dimension of the exit slit was normally 0.254 mm, but for the thermopile data was opened to 5.36 mm.

The optical path starting from the output slits of the monochromator, where the thermopile determination of the light power was made, consists of about 55 cm of air to the sapphire window of the vacuum chamber, through a quartz prism with an aluminized reflecting surface, and then to the sample. The thermopile also had a quartz window, and so should mostly cancel any effects due to variation in the transmission coefficient of the quartz prism. The air can be considered essentially 100% transmitting for wavelengths and path lengths involved in this experiment. The sapphire window transmission coefficient was measured on the Cary 15 spectrophotometer and is shown in Figure 7. The data are corrected for this variation in transmission. The reflectivity of the aluminum has been determined (20), and is constant to within one percent in the wavelength range of interest here, so is not corrected for.

B. Intensity vs Wavelength of Incident Light

As already mentioned, a Reeder thermopile, blackened for use in the ultraviolet, was used to determine the power distribution of the light from the monochromator. Its sensitivity is essentially constant throughout the wavelength range encountered in this experiment (30), so no separate determination of its response vs wavelength is necessary. These measurements were made with the thermopile window right next to the output slits of the monchromator. These slits were opened from their normal width (0.254 mm) to full width (5.36 mm) in order to increase the output signal of the thermopile. This does not change the pass band of the monochromator since the slit separation is held constant.

The output voltage of the thermopile was measured with a Keithley 148 nanovoltmeter, and recorded on a Varian Associates G11-A strip-chart recorder. The 0.1 μv and 0.3 μv scales of the nanovoltmeter were used. For each monochrometer position setting, the light was chopped at 1/30 Hz, and from 4 to 16 cycles of the output were recorded. This procedure was necessary in order to get the required precision (one percent) due to drift and noise in the thermopile output. Some reduction in these random fluctuations was achieved by wrapping the thermopile housing with layers of cloth and aluminum foil.

C. Photocurrent vs Wavelength

The photocurrent from the sample was measured with a Cary 31 vibrating reed electrometer and recorded on the G11-A strip-chart recorder. See Figure 8. The collection potential was provided by a fresh 22.5 v dry cell. This source was chosen after investigating the effects on the photocurrent of collection voltages ranging from 1.5 v to 60 v, from various chemical cells and from electronic power supplies. Most of the approach to the saturated photocurrent took place in the 1.5 to 12 volt range. There was about a three percent increase in the current in raising the collection voltage from 22.5 to 60 volts, but 22.5 volts were definitely on the plateau of the curve. The electronic supplies were found not to be sufficiently stable for use, and other cells are more expensive, but no quieter. (Several different mercury cells were also tried here.)

Two collection resistors were used; one was 10^{10} ohms and the other 4.8×10^{10} ohms. No change in the shape of the yield curves could be detected upon interchange of these resistors. The 10^{10} ohm resistor gave a faster response speed of the electrometer. Most of the data, however, were taken using the 4.8×10^{10} ohm resistor before this was discovered.

The procedure for taking photocurrent data was first to warm up the electronic systems for at least one hour. Just before current

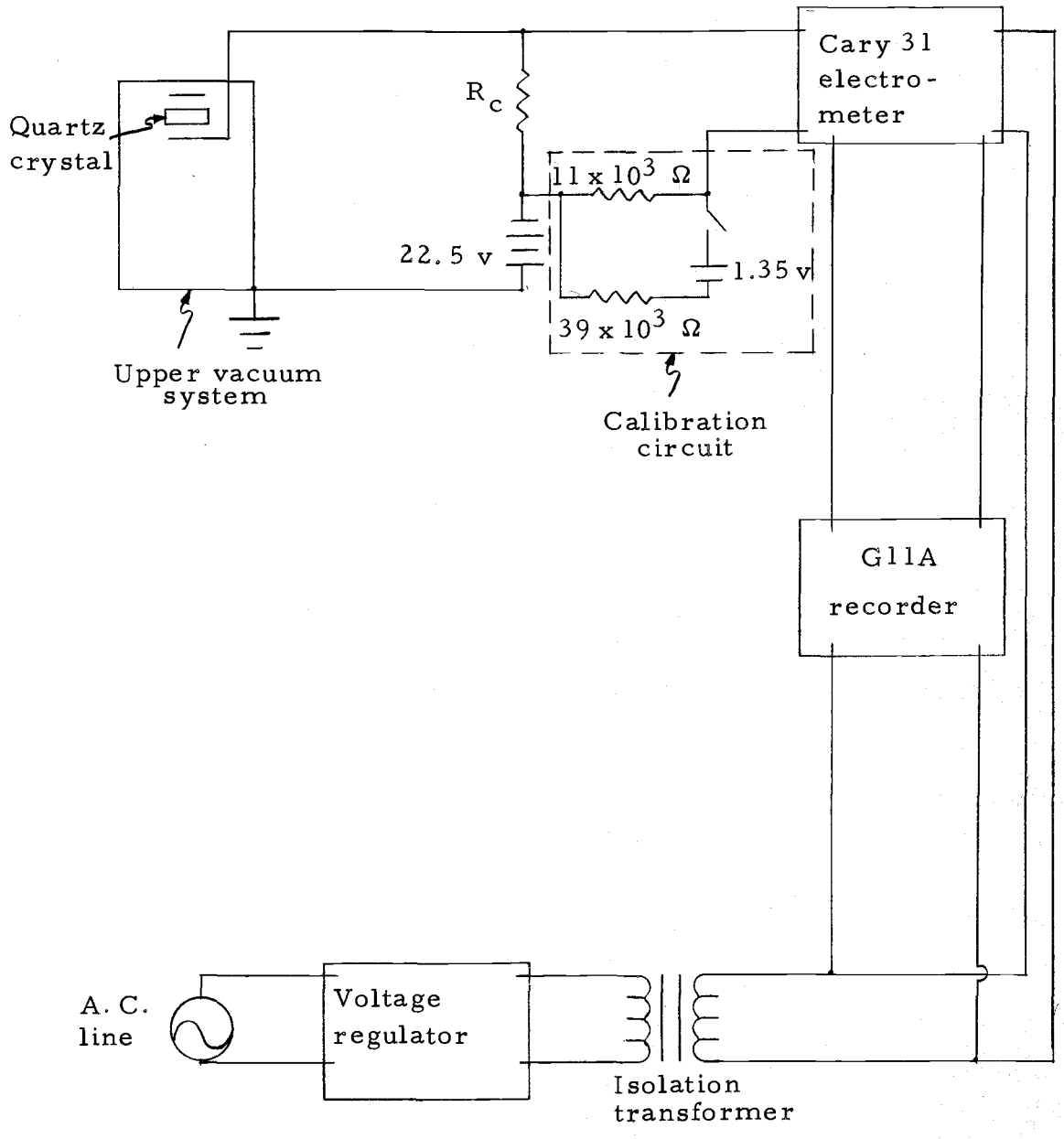

Figure 8. Photocurrent measuring system. R_c is the collection resistor, and had a value of 10^{10} Ω or 4.8×10^{10} Ω. The electrometer and recorder were operated in grounded enclosures to prevent electrical pickup.

measurements were begun, the electrometer and recorder calibration were checked by putting 0.3 v from a mercury cell across the electrometer input. The electrometer reading on the 300 mv scale was recorded, and the recorder was adjusted for a full scale deflection. Any changes in the mercury cell, electrometer, or recorder could then be detected and corrected for, so that data taken at different times could be compared. Observations of electrometer noise and drift on the 3 mv scale were then taken with the light turned off (by means of a chopper), and when sufficient stability was reached, the monochrometer was set to a position of 65 (3056 Å), with all filters removed, and the light was turned on. When a constant current was reached, the monochrometer p.s. was changed to 66, and so on, until the readings reached near full-scale, at which time the light was turned off (with the chopper) and the zero level was checked for drift, while the electrometer scale was changed. The lamp current was checked and adjusted, if necessary, at this time, also. When the monochromator p.s. reached 105 (5060 Å), the CS3-72 filter was inserted, and the p.s. was set back to 100 (4810 Å), in order to match filtered and unfiltered data. Data taking was then continued to as long a wavelength as possible, determined by the criterion that the signal was about twice the noise. This usually meant that the final readings were taken on the 1 mv scale.

In order to take these data, it was necessary to float the electrometer and recorder above ground by about the collection potential. This was achieved by means of an isolation transformer between the a.c. line and the instruments. For quiet operation this necessitated placing the recorder and electrometer in grounded, shielded enclosures. Also, in order to achieve stable operation, the resistance between the input to the electrometer and ground had to be high. It was measured with a Keithley 600 A electrometer. Normally, this resistance was greater than 10^{13} ohms, the highest resistance the 600 A could read. Under these conditions, the Cary 31 was relatively stable and quiet. If the liquid nitrogen reservoir was allowed to run dry and warm up, the noise signal of the Cary 31 gradually increased over a period of about two weeks, at which time the photocurrent was completely obscured by the noise. This effect was only slightly noticeable after two days at room temperature. After this two week period, the resistance to ground had decreased into the 10^{12} ohm range. After baking the system out at 220°C for 12 hours, with the system still at room temperature, the original low noise and high resistance to ground was restored, but the photocurrent had completely disappeared, due to evaporation of the sample (potassium). An explanation may be that the potassium at room temperature gradually diffuses over the quartz surface to a portion of the holder, which is connected to ground. This provides leakage paths from the

electrode upon which the deposits are made, and which is connected to the electrometer input, to ground. The shortest path distance from the edge of the original deposit to a grounded portion of the holder is about 2.8 mm.

IV. RESULTS OF MEASUREMENTS

A. Photoelectric Yield for Clean Potassium

It was anticipated that the yield vs wavelength of light for pure potassium would have the same general shape and behavior as that of previous investigators, but perhaps a higher work function due to the pains taken to obtain a clean, uncontaminated surface, similar in kind to Whitefield's results on sodium (51). However, the work function of 2.395 ± 0.005 eV is right in line with other results using modern vacuum techniques, although near the top end of the range. Representative data are shown in the Appendix.

There were two other unanticipated results. First, in the neighborhood of the threshold, a Fowler plot exhibited what appears to be two thresholds. See Figure 9. That is, about the first decade of data, starting from the longest wavelength at which data was obtainable, fitted fairly well a Fowler plot with a certain assumed work function. Then there was a break in the data, and the next decade or two fitted a Fowler plot with a different (higher) assumed work function.

The double threshold might be explained by the presence of crystallites of two different orientations in the deposit. The difference in work function of 0.3 to 0.4 eV between the two threshold regions as exhibited by the Fowler plot is consistent with Lang and

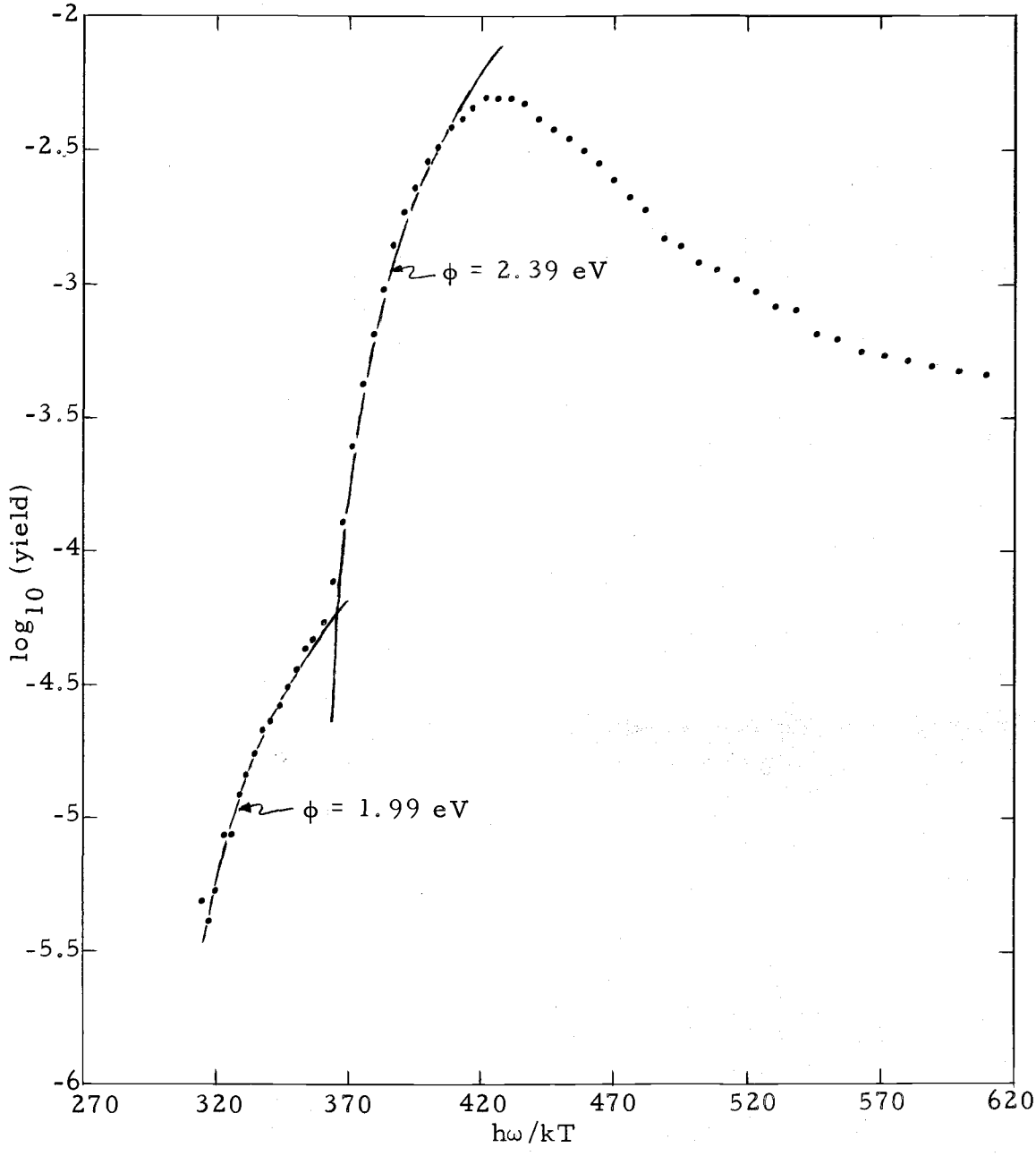

Figure 9. Fowler plot for pure potassium, showing the double threshold. The solid lines are best fits of the Fowler theory to the two threshold regions, giving work functions of 1.99 eV and 2.39 eV.

Kohn's theoretical determination of such differences. See Table 2. Also, the fact that the thick samples had the double threshold, while the thinner deposit did not is indicative that the deposition rate or thickness influence the phenomena, consistent with van Oirschot's data (50). There is also some evidence for hcp crystallites in the sample (25). Polymorphic transformations are the presumed causes of breaks in resistance vs temperature curves (29), one discontinuity occurring at about 78°K for potassium.

Table 2. Theoretical and experimental work functions (from Lang and Kohn (27)). Φ_u is the work function for the uniform-background model; $\delta\Phi$ is the first-order pseudopotential correction; $\Phi = \Phi_u + \delta\Phi$ (rounded to the nearest 0.05 eV). The pseudopotential core radii are r_c. Φ_{expt} are experimental values for polycrystalline samples. The most densely packed face of the bcc structure is (110).

	Na	K
Structure	bcc	bcc
r_s	3.99	4.96
Φ_i (eV)	3.06	2.74
r_c	1.67	2.14
$\delta\Phi$ (eV)		
(110)	0.03	0.01
(100)	-0.29	-0.34
(111)	-0.39	-0.40
Φ (eV)		
(110)	3.10	2.75
(100)	2.75	2.40
(111)	2.65	2.35
Φ_{exp} (eV) (polycrys.)	2.7	2.38

Another possibility, as put forth in explanation of the same phenomena in sodium (16) and rubidium (38), is the existence of surface states in the gap between the Fermi level and the vacuum level. The location and density of these states would be dependent on conditions at the surface, and would thus depend on deposition techniques, also. The fact that the density and location of these states does not change significantly with time in this experiment, as the yield at the peak does, would seem to favor the two-orientations of crystallites explanation. This is based on the interpretation of the change of the yield with time at the surface plasmon energy as being due to a decrease in roughness of the surface as the potassium atoms diffuse. This change in surface configuration would cause a change in the surface potential, and thus a change in parameters effecting the surface states (8, 18, 21, 31, 48). However, it is also possible that the diffusion to a smoother surface would not involve a change in the parameter, such as the lattice constant, responsible for surface states, and so even though the surface plasmon-light coupling decreased, the surface states could remain about constant in density and location, maintaining the double threshold. It is known that adsorbates on the surface can quench surface states (8), and the disappearance of the double threshold when sulfur is added is consistent with this. Lack of information about the structure and composition of the surface prevents a definitive statement about the origin

of this double threshold.

The second surprise was the time dependence of the yield for pure potassium (Figure 10 and the Appendix). Other investigators (3, 5, 50) have seen a small change in the yield in the first few minutes immediately following deposition, followed apparently by a stable, time independent yield for sodium or potassium, deposited at room temperature or 77°K. The above statements refer to investigators who appear to have used good vacuum techniques, since it is well known that slight amounts of contamination will effect the yield of potassium significantly. However, this same contamination will also change the work function, and the location of the peak in the yield, neither of which effects were observed in the pure potassium data of this work, even after a week of observations on the same deposit.

The only other evidence in the literature of this kind of time dependence under similar conditions is for pure cesium (4). Using approximately the same techniques, the same group obtained a time-independent yield for pure potassium (3). Their cesium photoyield decreased by about 40% in the first 20 hours after deposition, and remained essentially constant after this, out to about 70 hours after deposition. They suggest contamination as a possible cause, but the work function is constant, as is the location of the peak, which would not be the case if contamination were occurring.

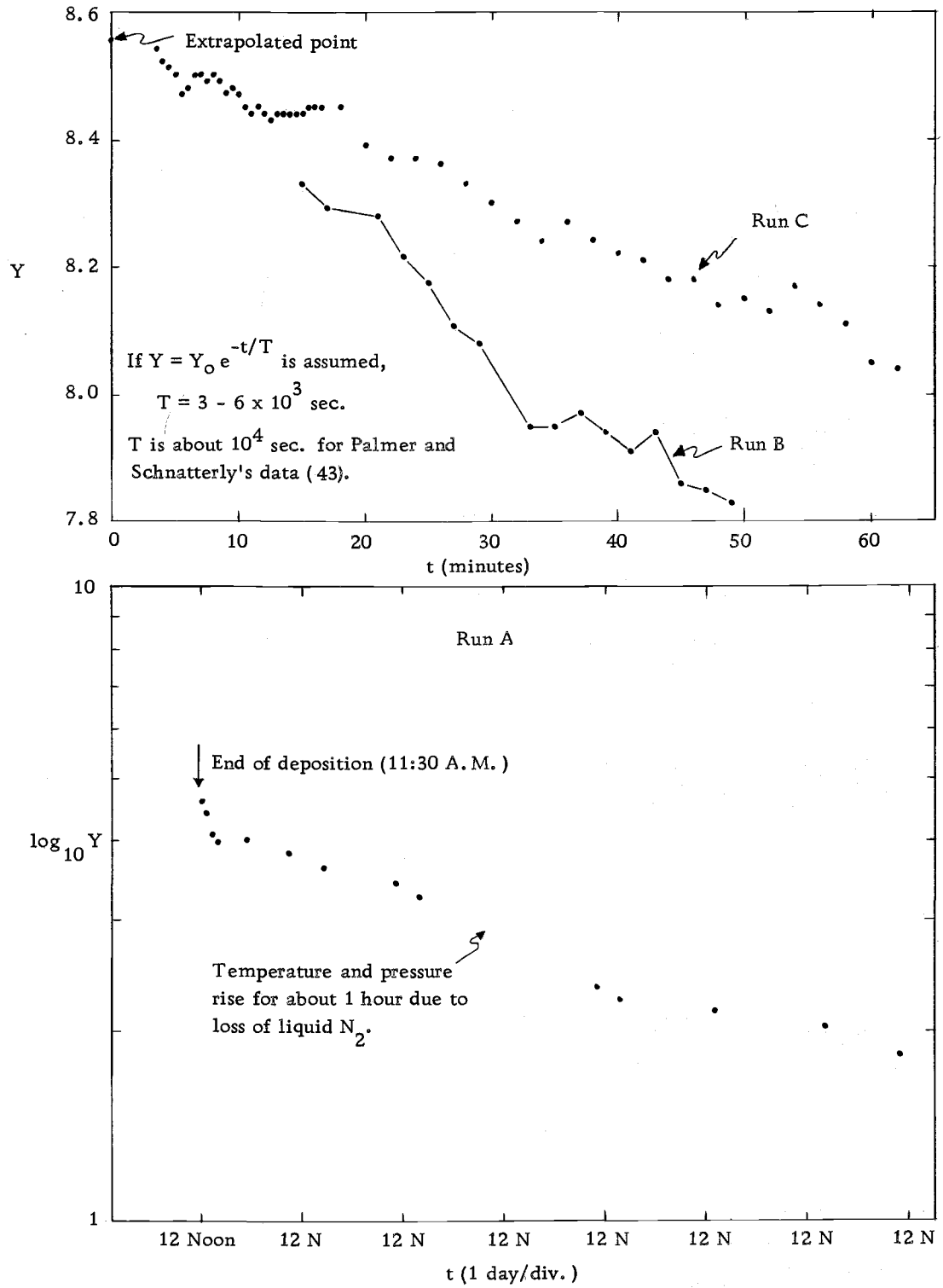

Figure 10. The upper figure is yield vs time, the lower one is $\log_{10}$ (yield) vs time for pure potassium held at 77° K. The end of the deposition occurs at time t = 0 in the upper figure.

What appears to be a related phenomenon is the time dependence in the optical data of Palmer and Schnatterly (43). One of their experimentally measured quantities, N, which is proportional to the imaginary part of the dielectric constant, exhibited a peak (actually two closely spaced peaks) at the surface plasmon frequency, which decayed at the same rate as the peak in the potassium yield data of this experiment. See Figure 10.

To further test the hypothesis that surface roughness is responsible for the surface plasmon peak, the yield at this wavelength was monitored as the liquid nitrogen evaporated, and the temperature of the sample rose. See Figure 11. The sharp break in this yield vs time plot would seem to be good evidence for the surface diffusion explanation, as explained in reference (43). As the temperature increases from 77°K, it is expected that a large increase in the self-diffusion rate will occur as the diffusion mechanism becomes activated. The fact that the yield rises after the initial drop is probably due to contamination. The pressure rises by a factor of about 100 during this warmup, due to release of material condensed on the liquid nitrogen well. The initial drop in the yield is probably not due to contamination, since the first bit of contamination is expected to increase the yield, and no such increase was observed. Palmer and Schnatterly (43) observe this kind of a drop in N at the surface plasmon peak when they allow their samples to warm up, also.

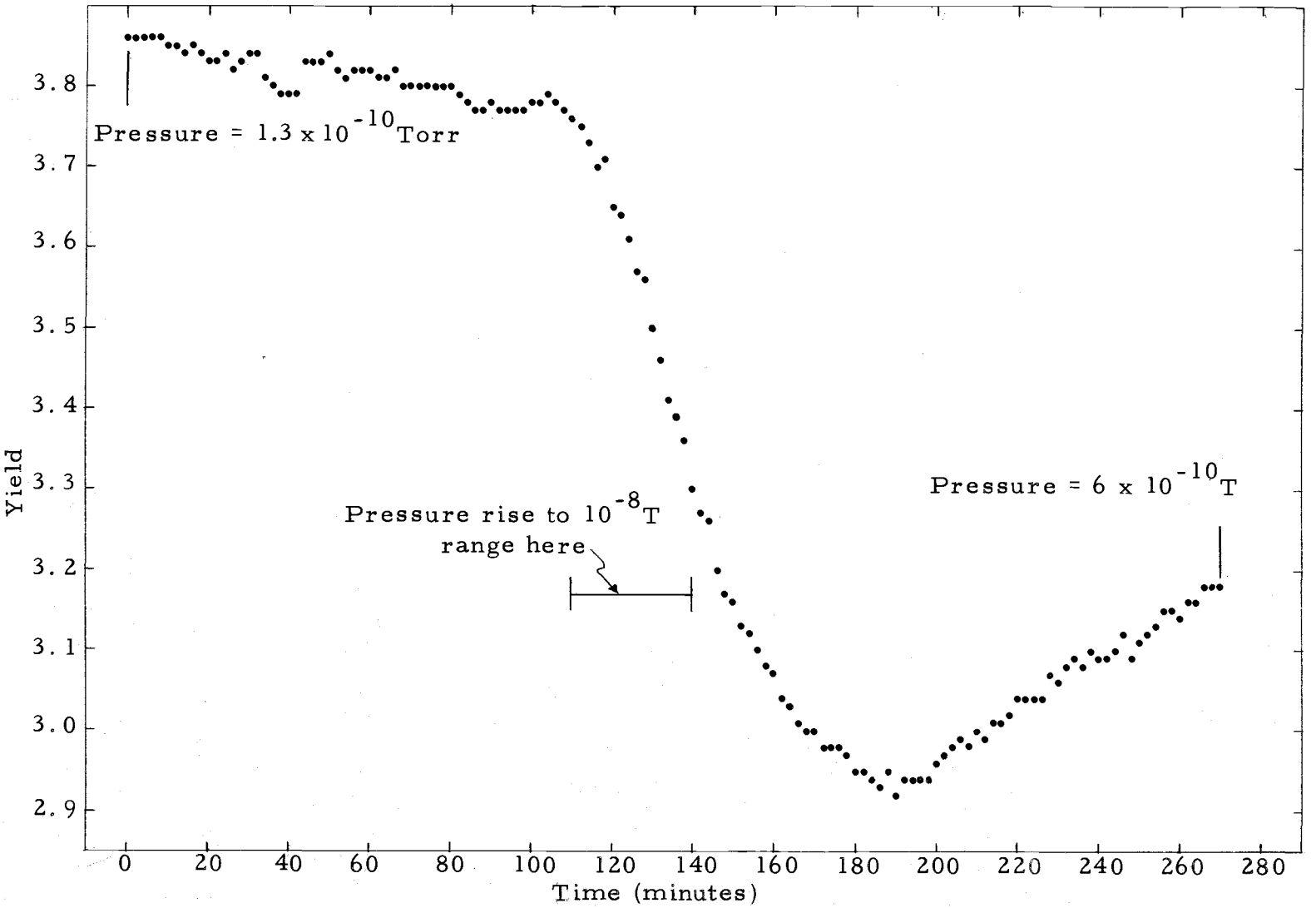

Figure 11. Yield vs time at the surface plasmon frequency, for pure potassium, as the temperature rises from 77°K.

B. Photoelectric Yield for Potassium with Various Coverages of Sulfur

There are five general types of effects that occur when small amounts of sulfur are added to a pure potassium deposition. First, the overall yield first increases up to about one monolayer of sulfur, and then decreases, and has almost disappeared at five monolayers. This is probably associated with the second effect in which the work function first decreases, out to about two monolayers, and then either increases slightly or remains about constant out to five monolayers. The location of the peak associated with the surface plasmon migrates as the sulfur coverage increases, from its initial value associated with pure potassium to a final, lower energy value, which remains about constant after approximately two monolayers of sulfur have been deposited. Fourth, the yield vs wavelength curve, which is originally mostly smooth, now becomes rough. A waviness of amplitude approximately five percent of the yield at that point is superimposed on a smoothed line drawn through the data. In sodium, this effect is not so pronounced, being only two percent or less. The last effect is the appearance at about 3.5 eV of what is interpreted as a second, broad peak, which does not really become well defined until about two monolayers of sulfur are deposited. This second peak did not show up in the sodium data but it may be that its presence was obscured by the migration of the surface plasmon-associated peak to about the

same energy region.

In order to investigate the origin of the second, sulfur-induced peak in the yield, a sample in which this peak was well-defined was followed as a function of time. This peak remained constant in time, while the surface-plasmon associated peak exhibited the same decay with time as it did for the pure potassium samples. This means that the sulfur-induced peak is probably associated with a bulk excitation process, in contrast to the surface plasmon peak.

In order to explain this sulfur-induced peak, a simple proposed energy-band model for the systems sulfur on potassium and sulfur on sodium is shown in Figure 12. The sulfur is assumed to be orthorhombic in form, and experimental and theoretical investigations of its energy band structure, in good agreement on the main features, have been carried out (6,7). Pure sulfur has a work-function of about 8 eV (7), so the proposed emission of electrons from sulfur at 3.5 eV light energy must be due to the interaction between the sulfur and the substrate. This interaction results in the matching of the Fermi levels in the substrate and the sulfur across their boundary. The Fermi level in the metal corresponds nearly to the highest filled level in the metal so the valence band in the sulfur has to rise in order that the metal and sulfur Fermi levels be the same. Figure 12 was drawn with the middle of the valence band 3.5 eV down from the vacuum level, to correspond with the peak in the photoyield at 3.5 eV, but the indicated

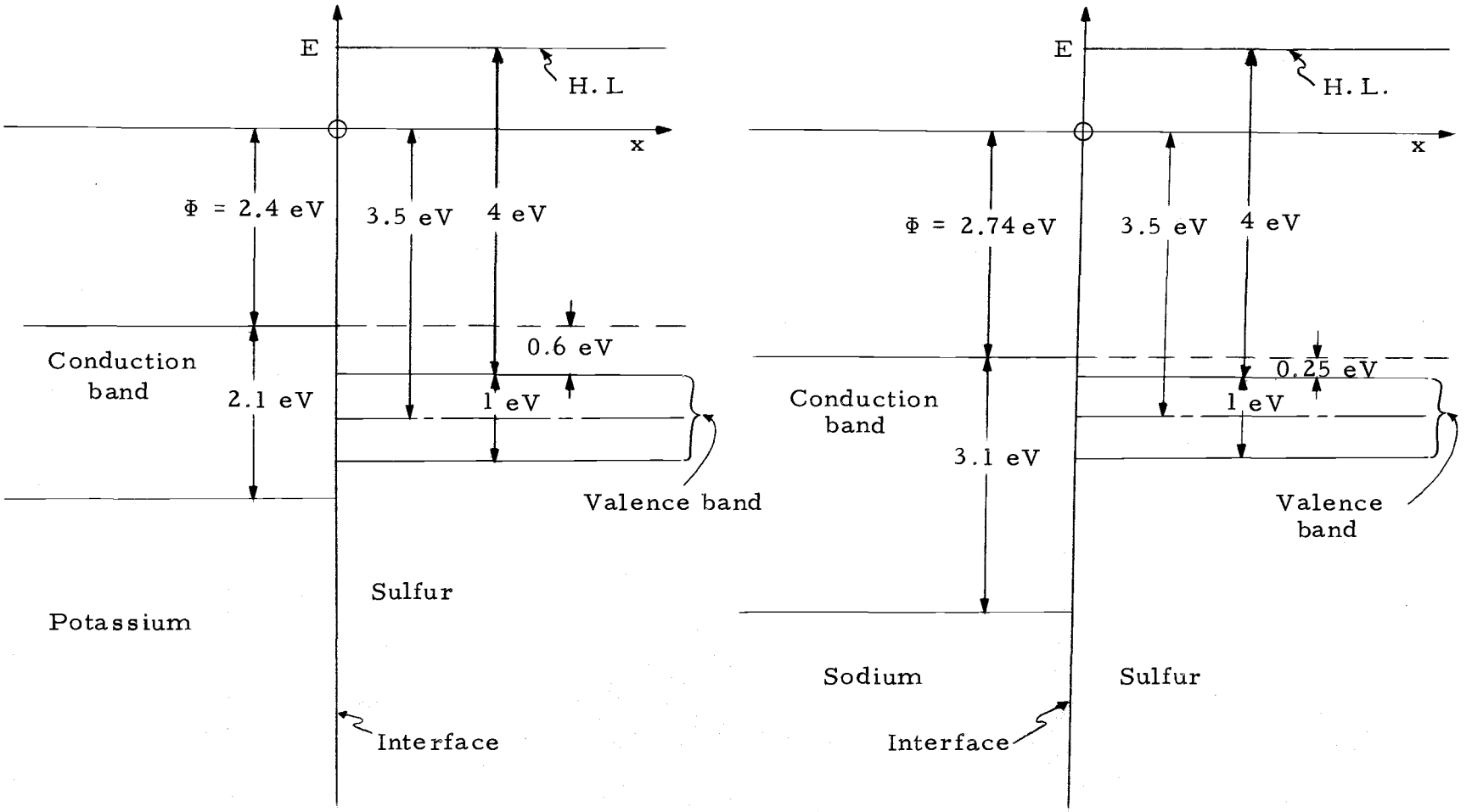

Figure 12. Energy vs distance along the surface normal for potassium and sodium with a sulfur layer, in a simplified representation. The sulfur bands are appropriate for the orthorhombic form, and band-bending is ignored. The work functions Φ in the figure are for pure potassium and sodium. For sulfur-contaminated substrates, the work functions are reduced to a minimum of about 2 eV. H.L. is a hopping level (7).

sulfur valence band actually consists of four overlapping bands (6) with an undetermined density of states, so the actual peak in the density of states, which should correspond to the peak in the photo-yield, is not known.

For this model, solutions of the Schroedinger equation for an electron with energy slightly above the vacuum level are plane waves in the metal and vacuum, and damped waves in the sulfur. Thus, photoemission from the sulfur would involve excitation of an electron from an initial valence level, to a damped wave state, followed by tunneling to the vacuum. The matrix element for dipole transitions between the valence and damped states was calculated, using a 3p atomic wavefunction for the valence state, and is nonzero. Further calculations in this model were not made due to lack of knowledge about the initial density of states function. Also, a proper comparison between this theory and experiment could not be made without a determination of the energy distribution of the photoelectrons, which was not done.

An alternate explanation of the second, sulfur-induced peak involves the creation of a peak in the density of initial states at 3.5 eV below the vacuum level, through the interaction of the potassium conduction electrons with the new potential at the surface, created by the presence of sulfur atoms. The potassium electrons spill over into the region occupied by the sulfur, out to about

2.5 monolayers of sulfur, and thus sample the sulfur potential there. The appearance of this scattering resonance would depend on the energy relationship between the sulfur levels and the substrate levels. This relationship would probably be different for sulfur on sodium than it is for sulfur on potassium, possibly accounting for the presence of the second peak in the potassium data and its absence in the sodium data. The perturbation of the density of initial states caused by this interaction may also be responsible for the fine structure in the yield induced by the sulfur contamination.

A similar sort of an explanation has been discussed and a theory developed (44). The results are obtained in the form of a change in the photocurrent $\Delta j(E)$. $\Delta j(E)$ is the difference between the photocurrent with an adsorbate (of up to about 1 monolayer coverage) and without the adsorbate, for electrons with energy E. Again, since energy analysis of the photoelectrons was not done in this experiment, no direct comparison with this theory is possible. However, qualitatively, the theory predicts an antiresonance in $\Delta j(E)$ arising from a degeneracy between the unperturbed adsorbate level and the continuum of metal states. If there is no degeneracy, this theory predicts a Lorentzian contribution to $\Delta j(E)$ due to the adsorbate levels. This theory fits experimental data for CO on Ni as well as could be expected, due to uncertainties in certain parameters of the theory.

The surface plasmon resonant frequency ω_{sp} characteristic of a semi-infinite metal is related to the bulk plasmon resonant frequency ω_p of the metal and the dielectric constant ϵ of an insulator occupying the other semi-infinite half-space by $\omega_{sp} = \frac{\omega_p}{\sqrt{1+\epsilon}}$. Table 3 gives experimental values for ω_p (25) and calculated values of ω_{sp}, assuming a vacuum ($\epsilon = 1$) outside the metal.

Table 3. Bulk plasmon (ω_p) and surface plasmon (ω_{sp}) frequencies for sodium and potassium.

	ω_p	$\omega_{sp} (=\omega_p/\sqrt{1+\epsilon})$
Potassium	3.8 eV	2.7 eV ± 0.1 eV
Sodium	5.8 eV	4.1 eV ± 0.1 eV

The peak in the yield vs wavelength curve for pure potassium in this experiment is at 2.85 eV ± 0.01 eV. Whitefield's value (49) of ω_{sp} for sodium is about 4.1 eV, the peak in his yield vs wavelength curves for pure sodium. As sulfur is added to the pure substrate, the peak in the curve gradually moves to lower energies, and remains about constant in energy with further sulfur deposition after about two monolayers. This lowered energy of the peak is 2.55 eV ± 0.05 eV for potassium in this experiment and 3.55 eV for sodium. If one uses the above equation to find the dielectric constant ϵ that would give this shift in ω_{sp}, one finds $\epsilon = 1.50$ for sulfur on potassium, and

$\epsilon = 1.67$ for sulfur on sodium. The value of ϵ for orthorhombic sulfur is about 4.0 (7). If one assumes $\epsilon = 4$, $\omega_{sp} = 1.70$ eV for potassium and $\omega_{sp} = 2.59$ eV for sodium. This is about 0.9 eV lower than the experimental values of the energy of the peak, and in the case of potassium is below the work function. This indicates that, although the surface plasmon excitation is a major contributor to the yield when its energy occurs above the threshold, and may even dominate the energy dependence in some regions, if this resonance occurs in the threshold region or below, its contribution will be dominated by the rapidly changing probability of finding an electron at that energy level, or the Fermi-Dirac function. The correspondence between the location in energy of the peak in the yield vs energy curve and the surface plasmon resonant energy would not be expected to be good when ω_{sp} is close to the work function.

Yield vs wavelength data are shown in the Appendix.

V. CALCULATIONS

A. $\delta\phi$ vs d

There has been much recent application of theoretical work to the variation of work function with adsorbate coverate (10, 15, 19, 22, 40, 42) in which the adsorbate is a metallic species, but very little for the case of a dielectric adsorbate. However, the recent theory of Lang and Kohn (27, 28) seems appropriate, and it is easy to apply.

To first order in perturbation theory, they derive an expression for the change in work function $\delta\phi$ in terms of a perturbation potential $\delta v(x)$, which is the perturbation potential $\delta v(r)$ averaged over the plane of the surface (y-z), and x is positive along the outward normal to the surface; and in terms of $n_\sigma(x)$, the density deficiency, which is given by

$$n_\sigma(r) = n_{N-1}(r) - n_N(r) ,$$

where n_N is the density distribution of N electrons in their ground state. It can be seen that

$$\int n_\sigma(r)dr = -1.$$

Also, in this model n_σ is taken to be a function of x only. With

these assumptions, Lang and Kohn show that

$$\delta\phi = -\int_{-a}^{\infty} \delta v(x) n_\sigma(x) dx \; / \; \int_{-a}^{\infty} n_\sigma(x) dx,$$

where a is a length large compared with a screening length, but small compared with the thickness of the substrate.

Lang and Kohn (28) have given results for $n_\sigma(x)$ using their self-consistent technique, as shown in Figure 13, but one still needs some expression for $\delta v(x)$ in order to use the above theory. First, orthorhombic sulfur is a good insulator with a gap of about 5.2 eV (7) between the top of the valence band and the bottom of the conduction band. The S_8 molecule, which is the assumed deposition species, has a similar gap between its highest occupied and lowest empty levels, and one might assume from this that the sulfur would look effectively to the free electrons in the substrate as a large positive potential. See Figure 12. There will also be band-bending effects due to the interaction between the substrate and the sulfur, and this was accounted for approximately by superimposing on the constant positive potential V_1 a potential of the form

$$V_2(x) = V_{20}(x-x_f)/(x_f-x_0) ,$$

so that $\delta V(x) = V_1 + V_2(x)$. V_{20} and V_1 were adjusted for a best fit to the data, and x_f was fixed so that V_2 went to zero at the

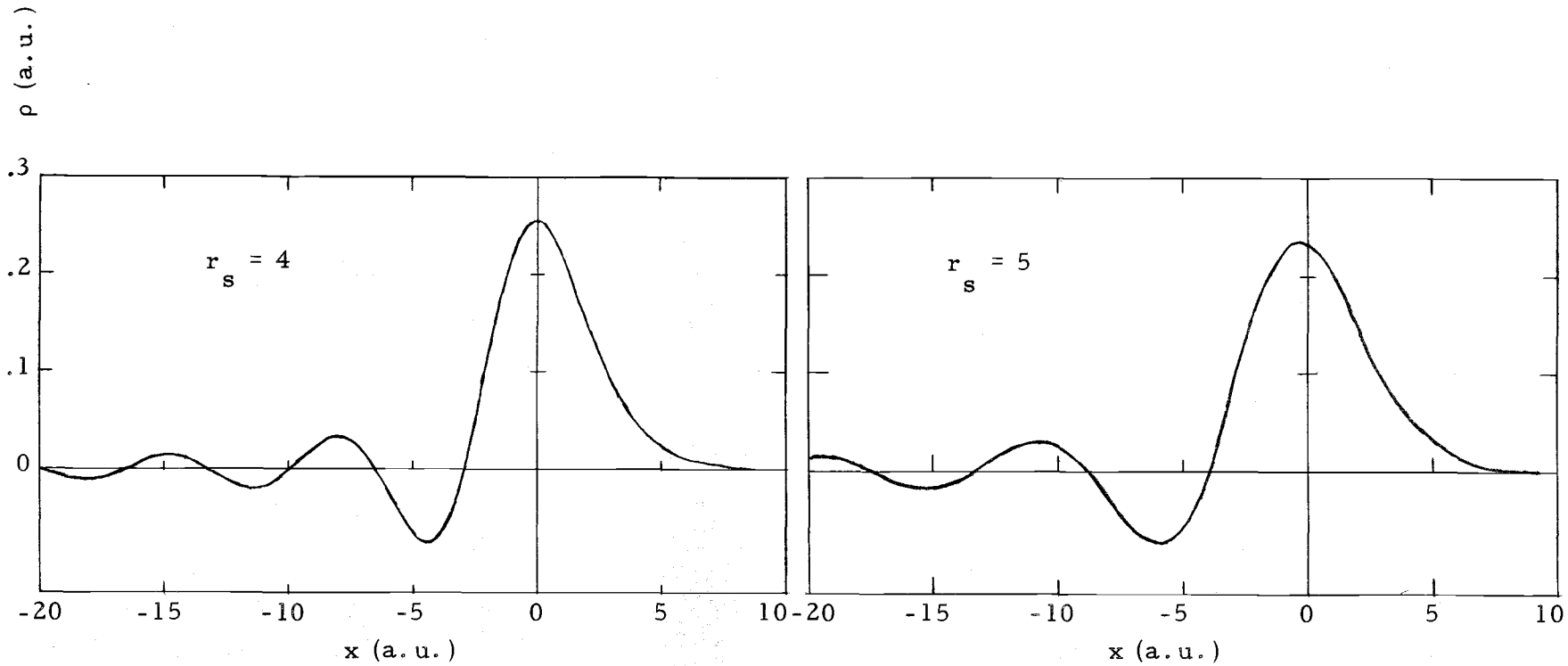

Figure 13. Induced surface charge density (proportional to n_σ). ρ and x are in atomic units (a.u.). The atomic unit of length is 0.529 Angstroms. From Lang and Kohn (28). The $r_s = 5$ curve, appropriate for potassium, is obtained by interpolation between the $r_s = 4$ and $r_s = 6$ curves shown by Lang and Kohn. The $r_s = 4$ curve is appropriate for sodium.

same position that $n_\sigma(x)$ did, since the metal's influence on the band structure of the sulfur was not expected to extend beyond the range of the metal's free electrons.

The location of the first sulfur molecule with respect to the surface was determined knowing the thickness of sulfur at which ϕ reached its minimum or constant value. This distance was then subtracted from the value of x at which $n_\sigma(x)$ went to zero to give the location of the beginning of the deposit, x_0.

The calculation was done by varying V_1 and V_{20} until the best least-squares fit to the data was obtained, using the constraint that the theoretical value of $\delta\phi$ where $n_\sigma = 0$ is equal to the experimental value of $\delta\phi$ at the minimum of the $\delta\phi$ vs d curve.

The results of these calculations and comparison with the experimentally determined values of $\delta\phi$ are shown in Figures 14 and 15.

It is obvious that this theory cannot predict any increase in ϕ beyond its minimum, since $n_\sigma(x)$ is monotonically decreasing beyond about $x = 0$, and, in fact, this theory predicts a constant work function no matter how much sulfur is added beyond about three angstroms. It seems that the reason for this discrepancy must arise because of the way the work function is measured. The Fowler theory requires that one extract and measure the photocurrent from electrons in an energy range inside the metal only slightly above the work

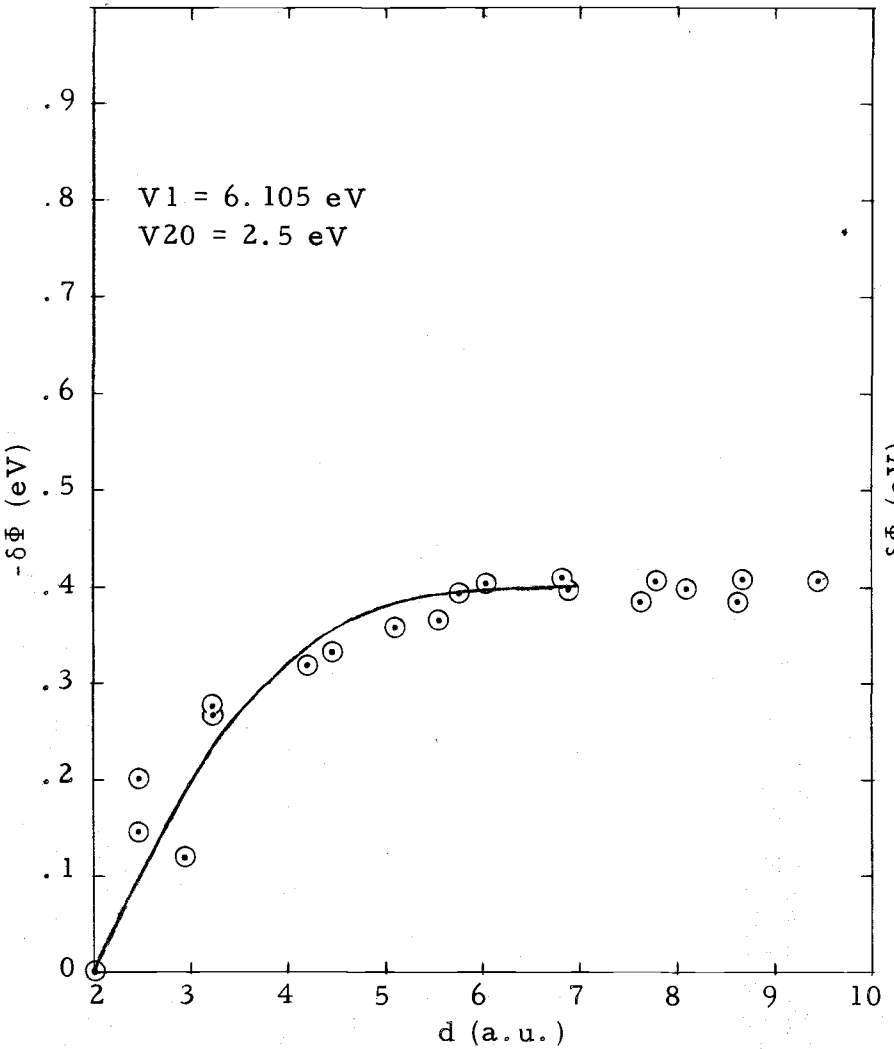

Figure 14. Change in work function vs sulfur thickness for a potassium substrate.

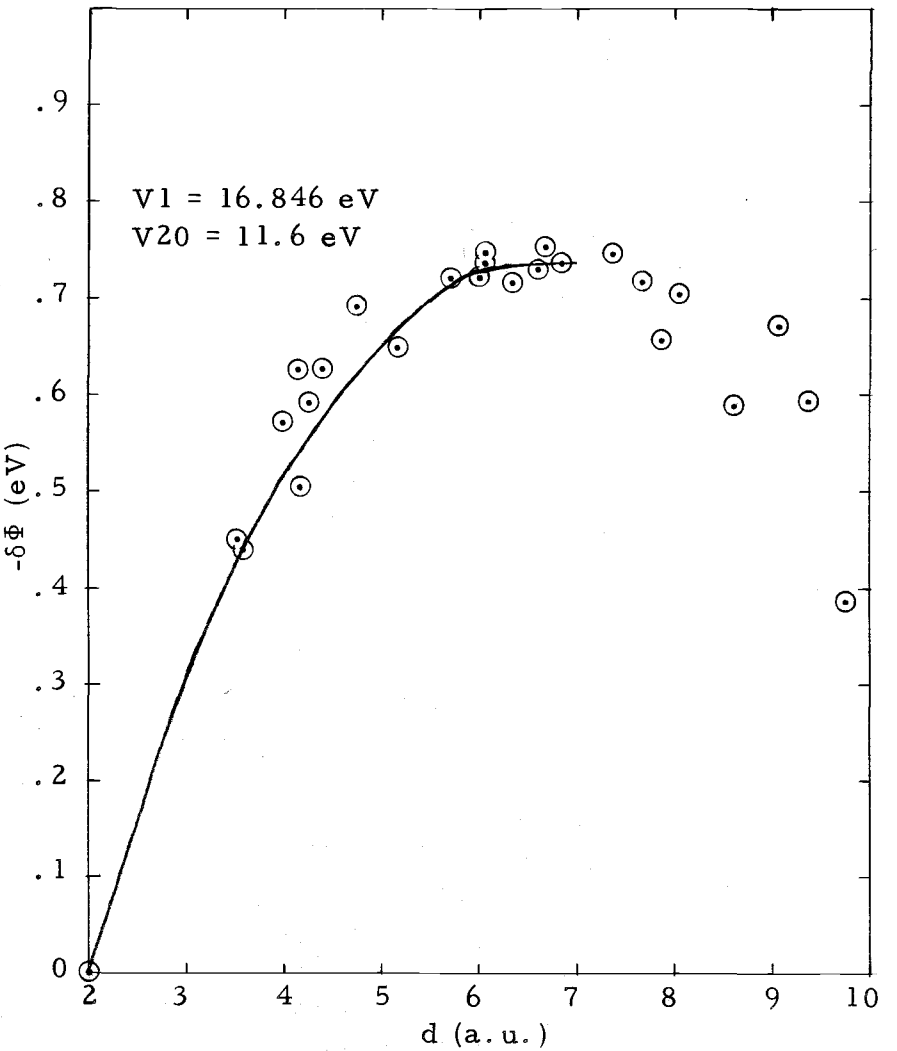

Figure 15. Change in work function vs sulfur thickness for a sodium substrate.

function, since that is where its assumptions are valid. However, as sulfur is added, these electrons see a higher (initially) and wider barrier which they must penetrate, and so one gradually loses just those electrons one needs to determine the work function by the Fowler theory, so that an apparent increase in the work function as sulfur is added beyond about three angstroms (one monolayer) is not surprising.

B. Light Absorption Coefficient for Sodium and Potassium with Various Sulfur Coverages

To get some idea of where the light energy is going in terms of transmission, reflection, and absorption coefficients, for the purpose of a possible explanation of the second, sulfur-induced peak in potassium, and its apparent absence in sodium, a theoretical analysis of the three component system sodium or potassium, sulfur, and vacuum was carried out. The model was a semi-infinite substrate of sodium or potassium, with various thicknesses of sulfur placed uniformly and homogeneously on top of this, and light incident normally from vacuum. The fraction of the incident light reflected back into vacuum R, the fraction transmitted into, and thus absorbed by, the metal T, and the fraction absorbed by the sulfur A, were calculated according to the classical theory (2).

In order to do this analysis, the complex dielectric constants of the various components are needed. For sodium and potassium, the data of Palmer and Schnatterly (43) are used. As mentioned previously, they obtained data at liquid nitrogen temperatures, and it shows what appears to be a surface plasmon effect just as the photoemission data does. For sulfur, the data of Cook and Spear (7) on orthorhombic single crystals is used. This work was apparently done at room temperature, but as the orthorhombic form is the only stable one below room temperature, the main features should be retained at liquid nitrogen temperatures.

Following are the formulas used in this calculation. T and R are calculated from them, and then $A = 1 - T - R$ is used.

$$r = (r_{12} + r_{23} e^{2ib}) / (1 + r_{12} r_{23} e^{2ib})$$

$$t = (t_{12} t_{23} e^{ib}) / (1 + r_{12} r_{23} e^{2ib})$$

are the reflection and transmission coefficients, respectively. $b = 2\pi \sqrt{c_2}\, h L^{-1}$, where h is the thickness of the middle section (sulfur), L is the wavelength of the incident light.

$$r_{12} = (\sqrt{c_1} - \sqrt{c_2})/(\sqrt{c_1} + \sqrt{c_2})$$

$$r_{23} = (\sqrt{c_2} - \sqrt{c_3})/(\sqrt{c_2} + \sqrt{c_3})$$

$$t_{12} = 2\sqrt{c_1}/(\sqrt{c_1} + \sqrt{c_2})$$

$$t_{23} = 2\sqrt{c_2}/(\sqrt{c_2} + \sqrt{c_3})$$

The subscript 1 refers to vacuum, 2 refers to the sulfur, and 3 refers to either sodium or potassium (the substrate). $T = \mathrm{Re}[\sqrt{c_3}\,|t|^2]$, $R = |r|^2$ are the transmissivity and reflectivity, respectively. The dielectric constants c are obtained as mentioned above from experimental data, with $c_1 = 1$. T and R were then obtained using a computer program. The dielectric constant data were read from the published graph and the above equations solved for T and R at 0.125 eV intervals. The results of these calculations are shown in Figures 16 and 17.

There is absorption of light energy in the sulfur in the same region that the sulfur-induced peak in the yield occurs, although the precise shape of the two curves do not agree very well. Also, the light absorption in the case of a sodium substrate is two to three times that for potassium, at the absorption peaks. So that, if this light absorption in sulfur on a potassium substrate is responsible for the sulfur-induced peak, it is likely that there is a similar contribution to the sulfur-on-sodium photoemission.

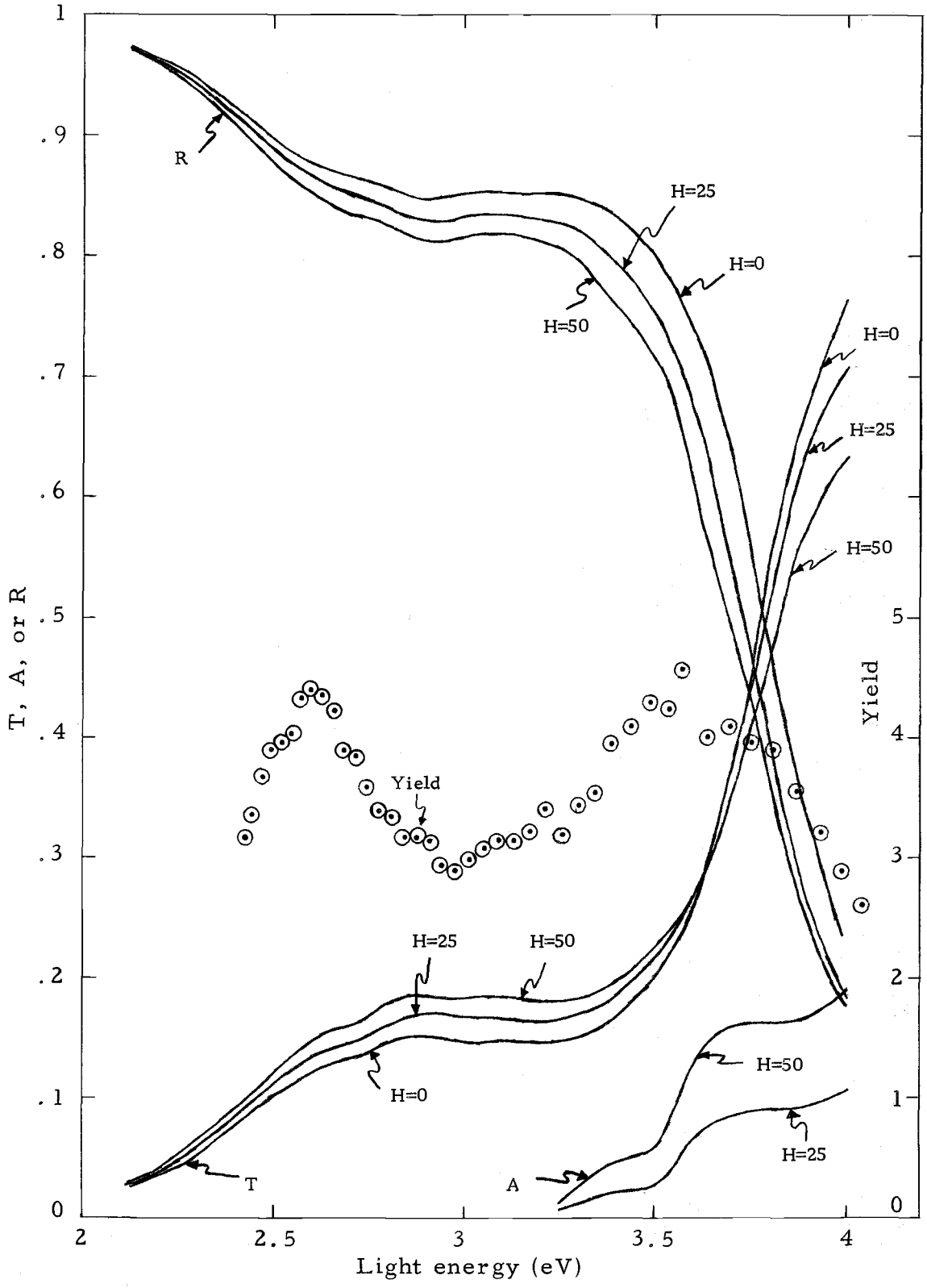

Figure 16. Light reflectivity R, transmissivity T, and absorptivity A for potassium with various thicknesses H (in angstroms) of sulfur on the surface. Also, yield for potassium with sulfur.

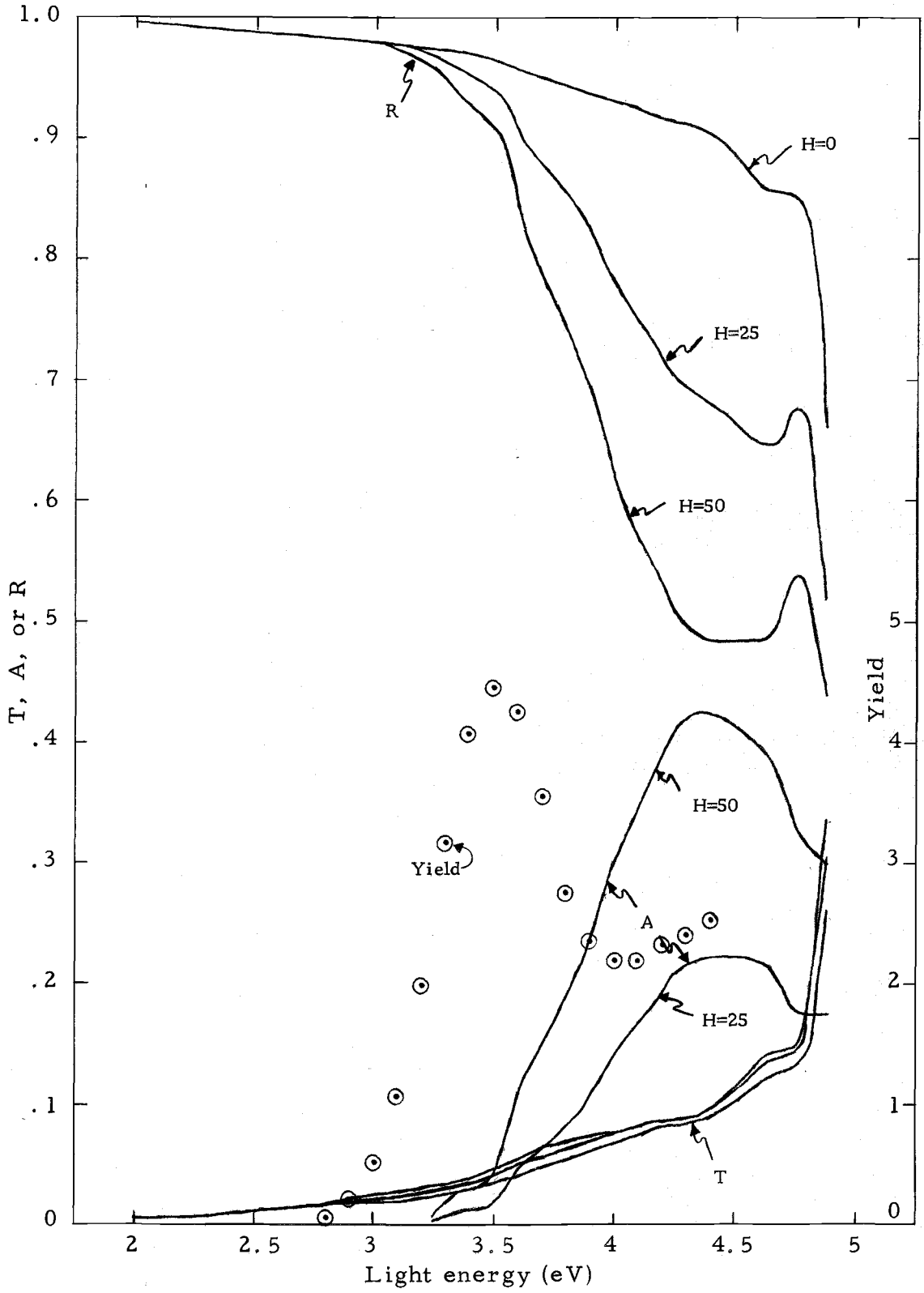

Figure 17. Light reflectivity R, transmissivity T and absorptivity A for sodium with various thicknesses H (in angstroms) of sulfur on the surface. Also, yield for sodium with sulfur.

C. Transition Probability for Light Absorption in the Sulfur Adsorbate

In order to investigate the suitability of one of the models (Figure 12) proposed to explain the sulfur-induced peak in the photoemission, the transition probability per unit time for dipole transitions between bound sulfur levels and the damped states of the substrate-sulfur-vacuum system which lie above the vacuum energy level, and may thus contribute to the photoemission, will be estimated here. The initial density of states is not known, but its strong energy dependence is expected to contribute most of the structure to the sulfur-induced peak in the photoemission. The width of the valence band, in which the initial states originate, is about 1 eV, which agrees approximately with the width of the observed sulfur-induced peak.

The valence band in orthorhombic sulfur arises from an appropriate combination of the 3s and 3p states of the atomic sulfur, so these 3s and 3p atomic states will be used as a rough estimate of the initial valence states of the sulfur.

$$\psi_{3s} = \{A+B(\frac{Zr}{a_o}) + C(\frac{Zr}{a_o})^2\}e^{-Zr/3a_o}$$

$$\psi_{3p} = \begin{cases} \{D(\frac{Zr}{a_o})+E(\frac{Zr}{a_o})^2\}e^{-Zr/3a_o}\cos\theta \\ \{F(\frac{Zr}{a_o})+G(\frac{Zr}{a_o})^2\}e^{-Zr/3a_o}\sin\theta\, e^{\pm i\phi} \end{cases}$$

$$Z = 6, \quad a_o = 0.529 \times 10^{-10}\text{m}.$$

The final state in this model is a damped state, of the form

$$\psi_f = (Ke^{\gamma z}+Le^{-\gamma z})\psi_f(\rho) = \psi_f(z)\psi_f(\rho) ,$$

where $\gamma^2 = (\frac{8\pi^2\mu}{h^2})(V_1-E)$, μ is the mass of an electron, V_1 is the potential an electron experiences in the sulfur, measured with respect to the vacuum level, and assumed to be positive, and E is the final state energy of the electron, assumed to be less than V_1. $0 < E < 1$ eV is the range of energies that is expected to contribute to the sulfur-induced peak. The z-direction is positive along the outward normal to the substrate surface. ρ is a coordinate in the x-y plane, and $\psi_f(\rho) = e^{i\vec{k}\cdot\vec{\rho}}$. The probability per unit time of absorption by dipole transitions of a photon of frequency $\omega_k = (E_f-E_i)/\hbar$ coming to the atom from any direction and with any polarization is given by

$$P_k = \frac{\omega_k^3}{hc^3}\sum_{\lambda}\int d\Omega_k |\langle\psi_f|\vec{M}\cdot\vec{\pi}_k^{\lambda}|\psi_i\rangle|^2 ,$$

where

$\vec{M} = e\vec{r}$, $\vec{r}$ the location of the electron which absorbs the photon.

$\vec{\pi}^1_k = \hat{x}$, $\vec{\pi}^2_k = \hat{y}$, are the two polarizations for light incident along the negative z axis.

$$d\Omega_k = \sin\theta\, d\theta\, d\phi$$

$$\vec{M}\cdot\vec{\pi}^1_k = er \sin\theta \cos\phi$$

$$\vec{M}\cdot\vec{\pi}^2_k = er \sin\theta \sin\phi$$

$$P_k = \frac{e^2\omega_k^3}{hc^3} \int d\Omega_k \sin^2\theta(\cos^2\phi + \sin^2\phi) |\langle\psi_f|r|\psi_i\rangle|^2$$

$$= \frac{8\pi}{3}\left(\frac{e^2\omega_k^3}{hc^3}\right) |\langle\psi_f|r|\psi_i\rangle|^2 \cong 10^{18} |\langle\psi_f|r|\psi_i\rangle|^2,$$

for $\hbar\omega = 3$ eV.

To evaluate P_k, one needs to find matrix elements M_i of several forms (the normalization of the wavefunctions is temporarily ignored at this point):

$$M_1 = \int d^3r\, e^{\pm\gamma z - i\vec{k}\cdot\vec{\rho}} r\, e^{-\delta r}, \quad \delta = \frac{z}{3a_o} = 3.8\ \text{Å}^{-1}.$$

$\vec{k}\cdot\vec{\rho} = kr\cos(\alpha-\phi)\sin\theta$, where α is the angle between $\vec{k}$ and the x-axis. The ϕ-integration will give Bessel functions, so one assumes $k = 0$, so that one can evaluate the matrix elements analytically. By looking at the current operator J_z, it can be seen that the

photoemission is independent of $\vec{k}$ in this model, anyhow.

$$M_1 \cong \int_0^{2\pi} d\phi \int_0^{\pi} d\theta \sin\theta \int_0^{\infty} dr\, r^3 e^{-\delta r \pm \gamma r \cos\theta},$$

where

$$\gamma^2 \cong 80 \times 10^{18}, \quad \gamma \cong 9 \times 10^9\, m^{-1} = 0.9\, \mathring{A}^{-1}.$$

$$M_1 \cong 2\pi \int_0^{\pi} d\theta \sin\theta\, (\delta \mp \gamma \cos\theta)^{-4} \int_0^{\infty} dv\, v^3 e^{-v}$$

$$= \frac{8\pi(3\delta^2+\gamma^2)}{(\delta^2-\gamma^2)^3}.$$

Matrix elements for the 3p states are zero. Matrix elements for the other parts of the 3s state introduce no significantly different features. No sharp structure in the energy dependence of the transition is introduced by this matrix element (M_1), in the energy region of interest. The magnitude of this matrix element (with the normalization constants of the wavefunctions reintroduced) would be of the order of atomic dimensions, so that $P_k \cong (10^{18})(10^{-10})^2 = 10^{-2}\ sec^{-1}$.

A typical value of the magnitude of the yield for the alkali metals is 1/200 electrons/photon, so that this transition rate is the right order of magnitude to make a sulfur-induced contribution to the photoemission of the same magnitude as for the pure metal. In order for an electron excited by this process to contribute to photoemission, it must tunnel out of the sulfur. Tunneling probabilities for insulators

of thickness 10 Å are of the order of 0.5, for electrons 1 eV above the vacuum level. Thus, insofar as the approximations and simplifications made in the above estimate can be reasonably accepted, there appear to be no strong objections to the above model, based on present data.

VI. DISCUSSION AND CONCLUSIONS

There are several contributions that this investigation makes. First, the successful application of Lang and Kohn's theory to the variation of work function of an alkali metal substrate with sulfur adsorbate thickness appears to be the first, although the possibility of such application, in general, has been mentioned.

Second, the appearance of a double threshold for some of the potassium depositions in this investigation tends to confirm its observation in other alkali metals (16, 38), and points to involvement of uncontrolled surface configuration variables in the photoemission data. This suggests a concurrent study of surface structure and composition by, say, low energy electron diffraction or Auger electron spectroscopy in conjunction with a photoemission experiment, in an attempt to determine the significant variables.

Third, the time dependence of the yield for pure potassium, in agreement with a time dependence of its optical properties, points out the importance of the surface plasmon in optical and photoemission properties. This involvement has been considered many times, but there does not appear to be any previously published data on this kind of time dependence of the photoemission from potassium.

The fourth contribution has to do with the relative magnitudes of the work function in this work and in Whitefield's, compared to other

investigator's values. The extreme care taken to achieve and maintain a clean sample of pure sodium in Whitefield's work, and the resulting high work function were taken as possible evidence for sample contamination in other work, where the work function has been considerably lower. However, using essentially the same techniques, we have obtained a work function for pure potassium in good agreement with other determinations. This, along with other results mentioned above, is taken as evidence that contamination is not the only possible explanation of the variations in work function observed, but that other undetermined surface configuration variables may play a role.

BIBLIOGRAPHY

1. Beaglehole, D. and O. Hunderi. Study of the interaction of light with rough metal surfaces. I. Experiment. Physical Review B 2:309-321. 1970.

2. Born, M. and E. Wolf. Principles of Optics, 2nd Revised Edition. New York, Pergamon Press, 1964.

3. Boutry, G.A., H. Dormont, R. Evrard and R. Perrin. Contribution a l'etude des proprietes photoelectriques du potassium pur, prepare et conserve dans l'ultravide. Comptes Rendus Academie des Sciences 261:383-386. 1965.

4. Boutry, G.A., R. Evrard and J.C. Richard. Contribution a l'etude des proprietes photoelectriques du cesium pur, prepare et conserve dans l'ultravide. Comptes Rendus Academie des Sciences 258:143-146. 1964.

5. Brady, J.J. The photoelectric properties of alkali metal films as a function of their thickness. Physical Review 41:613-626. 1932.

6. Chen, Inan. Molecular-orbital studies of charge-carrier transport in orthorhombic sulfur. II. Electronic states of the crystal. Physical Review B 2:1060-1069. 1970.

7. Cook, B.E. and W.E. Spear. The optical properties of orthorhombic sulphur crystals in the vacuum ultraviolet. Journal of Physics and Chemistry of Solids 30:1125-1134. 1969.

8. Davison, S.G. and J.D. Levine. Surface States. In: Solid State Physics. Volume 25. New York and London, Academic Press, 1970. pp 2-149.

9. Dickey, Jean. New aspects of the photoelectric emission from Na and K. Physical Review 81:612-616. 1951.

10. Dionne, G.F. Image force work function of dielectric layers. Journal of Applied Physics 44:5637-5638. 1973.

11. Elson, J.M. and R.H. Ritchie. Photon interactions at a rough metal surface. Physical Review B 4:4129-4138. 1971.

12. Endriz, J.G. Calculation of the surface photoelectric effect. Physical Review B 7:3464-3481. 1973.

13. Endriz, J.G. and W.E. Spicer. Study of aluminum films. II. Photoemission studies of surface-plasmon oscillations on controlled-roughness films. Physical Review B 4:4159-4184. 1971.

14. Felch, E.P. and J.O. Israel. A simple circuit for frequency standards employing overtone crystals. Proceedings of the Institute of Radio Engineers 43:596-603. 1955.

15. Flaim, T.A. and P.D. Ownby. Adsorbate-induced work function changes. Surface Science 32:519-526. 1972.

16. Garron, R., L. Gaudart and R. Payan. Proprietes optiques et photoelectriques des couches minces de sodium, en liason avec leur structure electronique. Comptes Rendus Academie des Sciences 268:266-269. 1969.

17. Grant, D.S. The theory of the surface photoelectric effect for alkali metals applied to potassium. Thesis, The Pennsylvania State University, 1971. Unpublished.

18. Gurman, S.J. and J.B. Pendry. Existence of generalized surface states. Physical Review Letters 31:637-639. 1973.

19. Gyftopoulos, E.P. and J.D. Levine. Work function variation of metals coated by metallic films. Journal of Applied Physics 33:67-73. 1962.

20. Hass, G. and J.E. Waylonis. Optical constants and reflectance and transmittance of evaporated aluminum in the visible and ultraviolet. Journal of the Optical Society of America 51:719-722. 1961.

21. Haydock, R. and M.J. Kelly. Surface densities of states in the tight-binding approximation. Surface Science 38:139-148. 1973.

22. Heine, V. and C.H. Hodges. Theory of the surface dipole on nontransition metals. Journal of Physics C: Solid State Physics 5:225-230. 1972.

23. Hunderi, O. Influence of grain boundaries and lattice defects on the optical properties of some metals. Physical Review B 7:3419-3429. 1973.

24. Hunderi, O. and D. Beaglehole. Study of the interaction of light with rough metal surfaces. II. Theory. Physical Review B 2:321-329. 1970.

25. Ichikawa, T. and S. Ogawa. Electron diffraction study of films of body-centered cubic metals condensed at low temperature. Japanese Journal of Applied Physics 7:1318-1323. 1968.

26. Kittel, C. Introduction to Solid State Physics. 2nd edition. New York, John Wiley and Sons, 1967. p. 234.

27. Lang, N.D. and W. Kohn. Theory of metal surfaces: work function. Physical Review B 3:1215-1222. 1971.

28. Lang, N.D. and W. Kohn. Theory of metal surfaces: induced charge and image potential. Physical Review B 7:3541-3550. 1973.

29. Lazarev, B.G., E.E. Semenenko and A.I. Sudovtsov. Polymorphic transformations of lithium, sodium and potassium in films condensed on a cold substrate. Journal of Experimental and Theoretical Physics 39:1165-1166. 1960.

30. Leighton, P.A. and W.G. Leighton. Some remarks on the use of thermopiles for the absolute measurement of radiant energy. Journal of Physical Chemistry 36:1882-1907. 1932.

31. Levine, J.D. Evaluation of surface-state theories. Physical Review 182:926-935. 1969.

32. Maissel, L.I. and R. Glang. Handbook of Thin Film Technology. McGraw-Hill Book Company, 1970. p. 1-21.

33. Makinson, R.E.B. Metallic reflexion and the surface photo-electric effect. Proceedings of the Royal Society A162:367-390. 1937.

34. Mayer, H., D.L. Blanaru and H. Steffen. Photoelectric and optical properties of thin alkali metal films. Thin Solid Films 5:389-406. 1970.

35. Meyer, B., Ed. Elemental Sulfur. New York, Interscience Publishers. 1965. 390 p.

36. Mitchell, K. The theory of the surface photoelectric effect in metals-I. Proceedings of the Royal Society A146:442-464. 1934.

37. Mitchell, K. The theory of the surface photoelectric effect in metals-II. Proceedings of the Royal Society A153:513-533. 1936.

38. Monin, J. Photoemission et proprietes optiques des metaux alcalins purs. Acta Electronica 16:139-173. 1973.

39. Mueller, R.M. and W. White. Direct gravimetric calibration of a quartz crystal microbalance. Review of Scientific Instruments 39:291-295. 1968.

40. Muscat, J.P. and D.M. Newns. Atomic theory of work function variation in alkali adsorption on transition metals. Solid State Communications 11:737-741. 1972.

41. Olpin, A.R. Method of enhancing the sensitiveness of alkali metal photoelectric cells. Physical Review 36:251-295. 1930.

42. Paasch, G. and J. Esching. Work function and surface structure of simple metals. Physica Status Solidi 51:283-293. 1972.

43. Palmer, R.E. and S.E. Schnatterly. Observation of surface plasmons and measurement of the optical constants for sodium and potassium. Physical Review B 4:2329-2339. 1971.

44. Penn, D.R. Photoemission spectroscopy in the presence of adsorbate-covered surfaces. Physical Review Letters 28:1041-1044. 1972.

45. Phelps, F.P., R.D. Goodwin and A.H. Morgan. Investigation of stability of quartz resonators at low temperatures. Boulder, Colorado, 1956. 58 p. (U.S. National Bureau of Standards. Report 5021).

46. Sauerbrey, G. Verwendung von Schwingquarzen zur Wagung dunner Schichten und zur Mikrowagung. Zeitschrift fur Physik 155:206-222. 1959.

47. Smith, N.V. and W.E. Spicer. Photoemission studies of the alkali metals. I. Sodium and potassium. Physical Review 188:593-605. 1969.

48. Steslicka, M. Note on the existence conditions of surface states. Physics Letters 44A:513-514. 1973.

49. Stockbridge, C.D. Vacuum Microbalance Techniques 5:193-205. 1966. Resonance frequency versus mass added to quartz crystals.

50. van Oirschot, G.J., M. van den Brink and W.M.H. Sachtler. Photoelectric emission and phase transitions of evaporated metastable sodium, potassium and sodium-potassium alloy films. Surface Science 29:189-202. 1972.

51. Whitefield, R.J. Surface effects in photoemission from sodium. Thesis, Oregon State University, 1970. Unpublished.

52. Whitefield, R.J. and J.J. Brady. Vacuum microbalance for 77.3°K operation. Review of Scientific Instruments 38:1670-1671, 1967.

53. Whitefield, R.J. and J.J. Brady. New value for work function of sodium and the observation of surface-plasmon effects. Physical Review Letters 26:380-383. 1971.

54. Wyckoff, R.W.G. Crystal Structures, 2nd edition. Volume 1, p. 16. Interscience Publishers. 1963.

APPENDIX

Following are some yield vs wavelength data. Figure 18 is for a pure potassium sample. The remaining plots are for a series of sulfur depositions. The number at the top in the middle of the page is the total change in frequency of the microbalance oscillator, corresponding to the total amount of sulfur deposited at that point. The number of monolayers (m.l.) of sulfur is also given. The wavelength λ in angstroms is related to the monochromator position setting (p.s.) by $\lambda = 50.1(\text{p.s.}) - 200$. Finally, there is a tabulation of work functions for pure potassium.

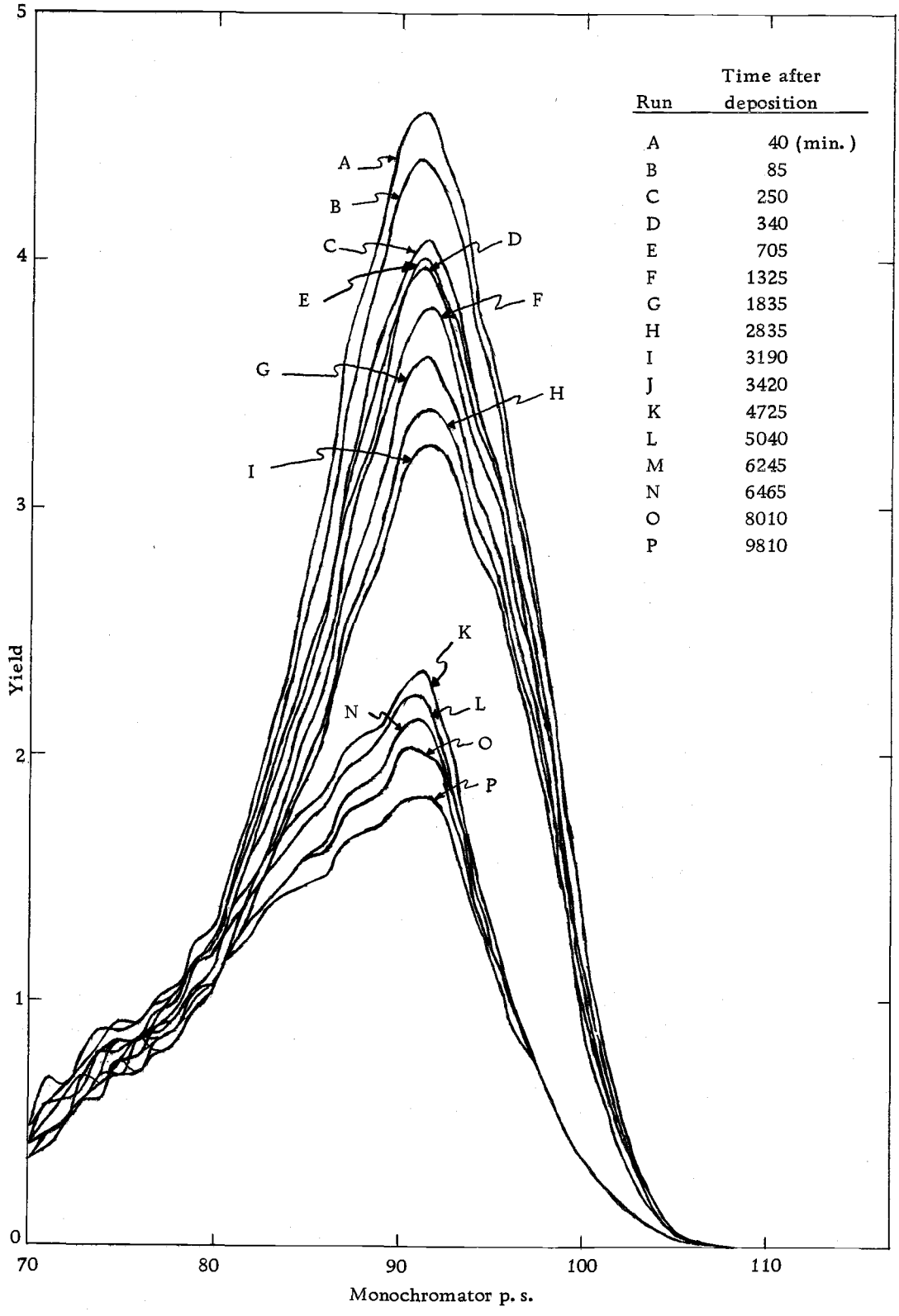

Figure 18. Family of yield vs wavelength curves, for different times after deposition. Runs J and M were begun, but not completed due to excessive noise in the photocurrent, of undetermined origin. Between runs I and J, the liquid nitrogen ran out for about one hour, allowing the temperature to rise somewhat. The work function and location of the peak are about constant throughout this series.

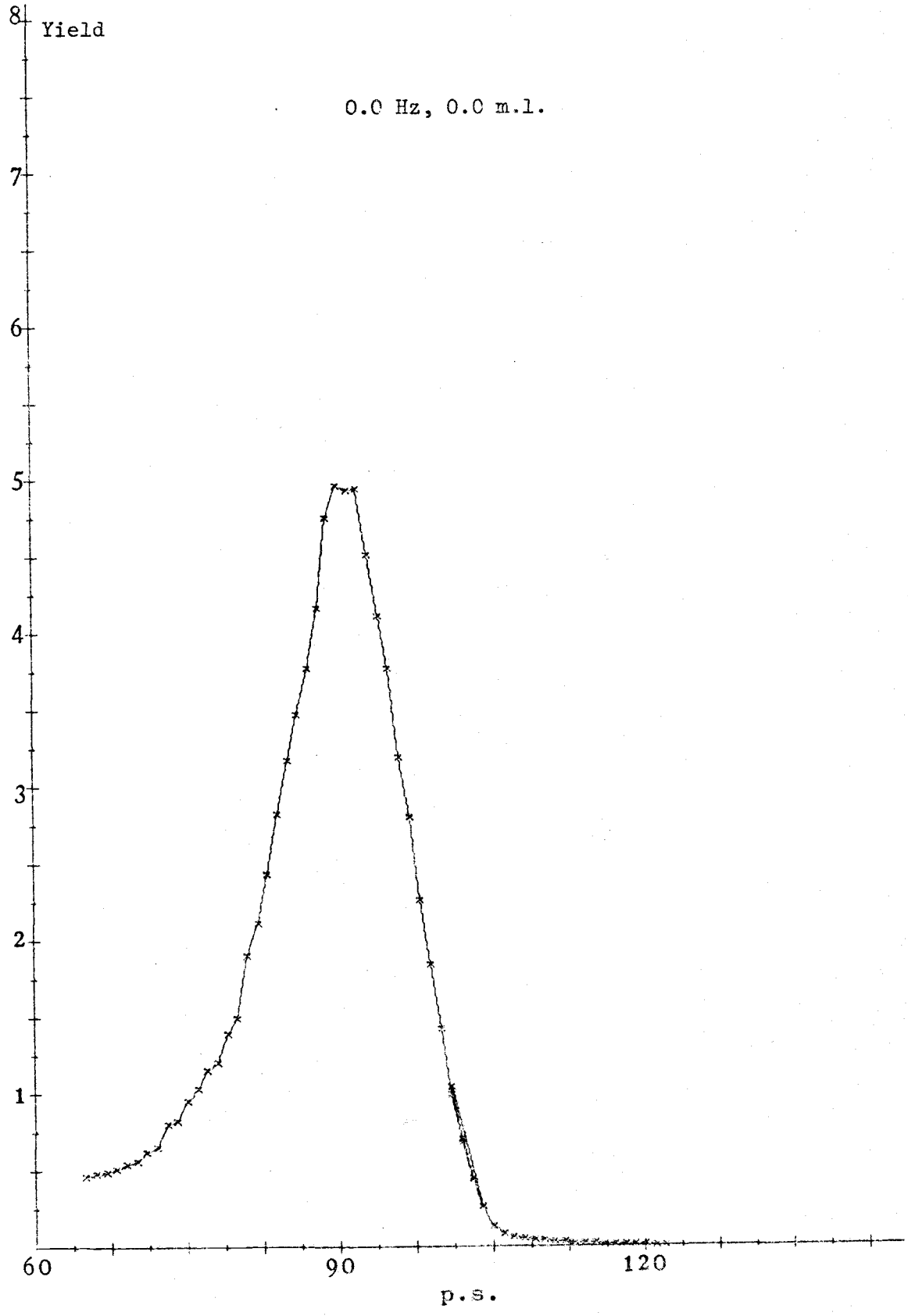
Yield
0.0 Hz, 0.0 m.l.
8
7
6
5
4
3
2
1
60
90
120
p.s.

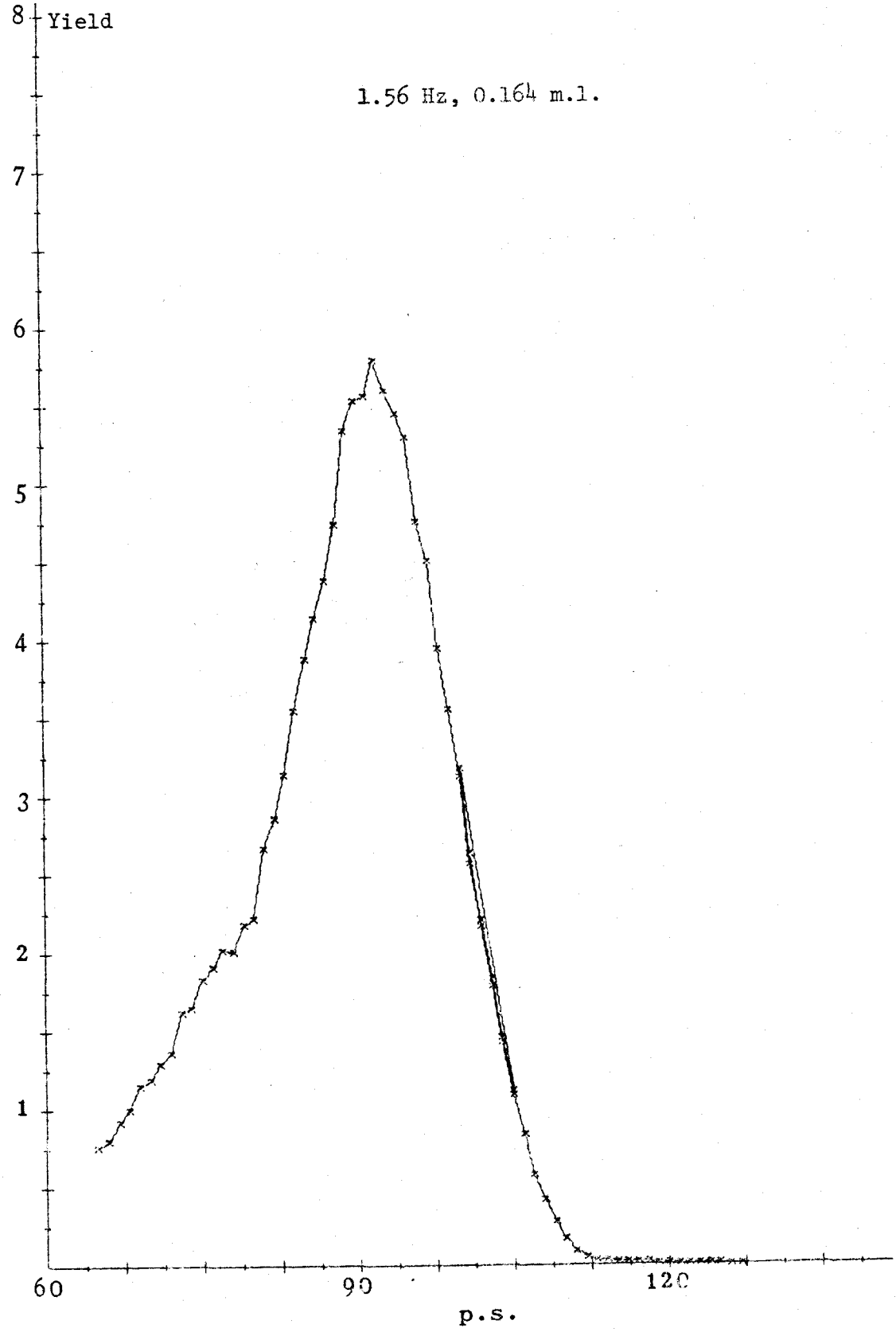
Yield
1.56 Hz, 0.164 m.l.
8
7
6
5
4
3
2
1
60
90
120
p.s.

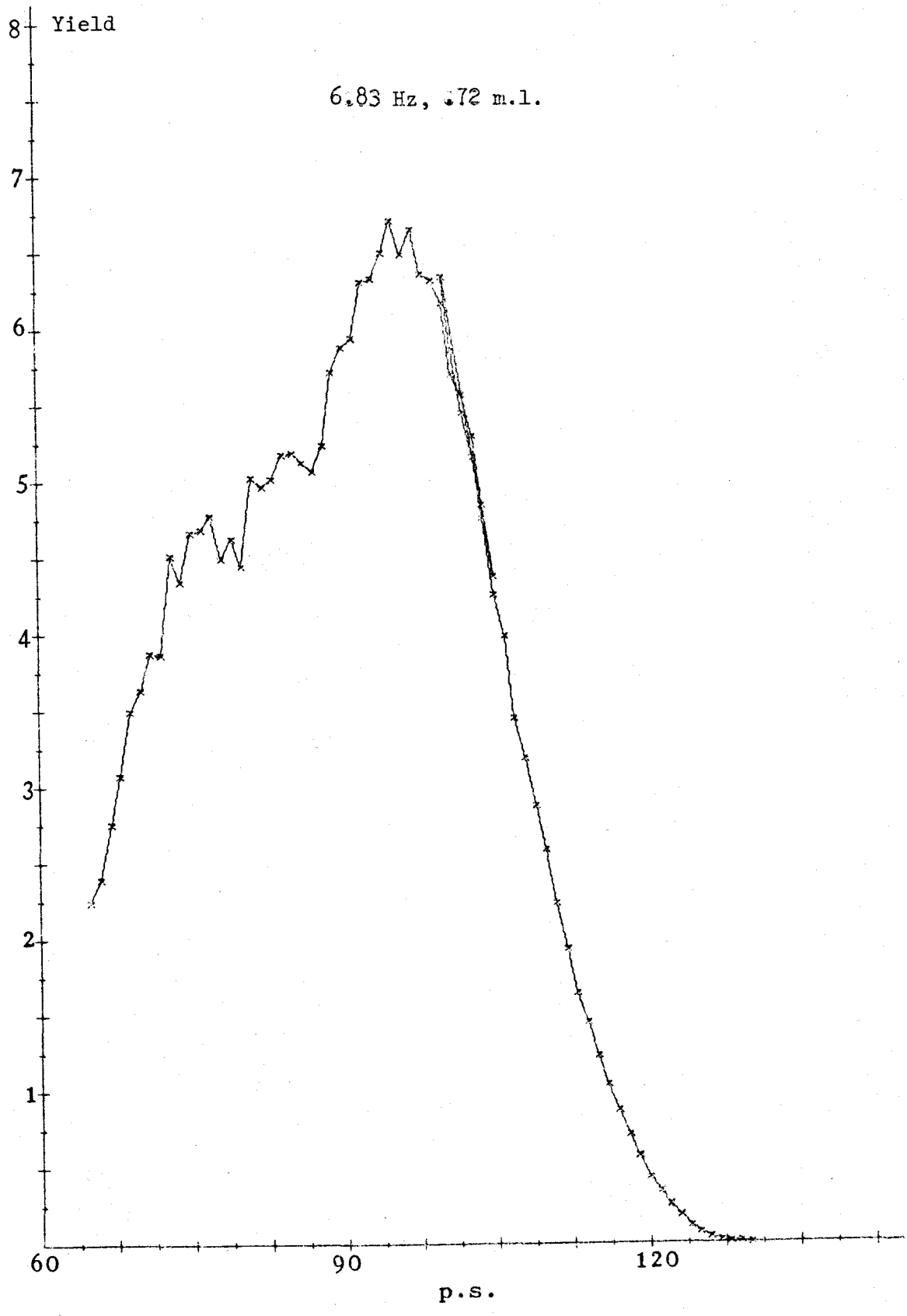
Yield
6.83 Hz, .72 m.l.
8
7
6
5
4
3
2
1
60
90
120
p.s.

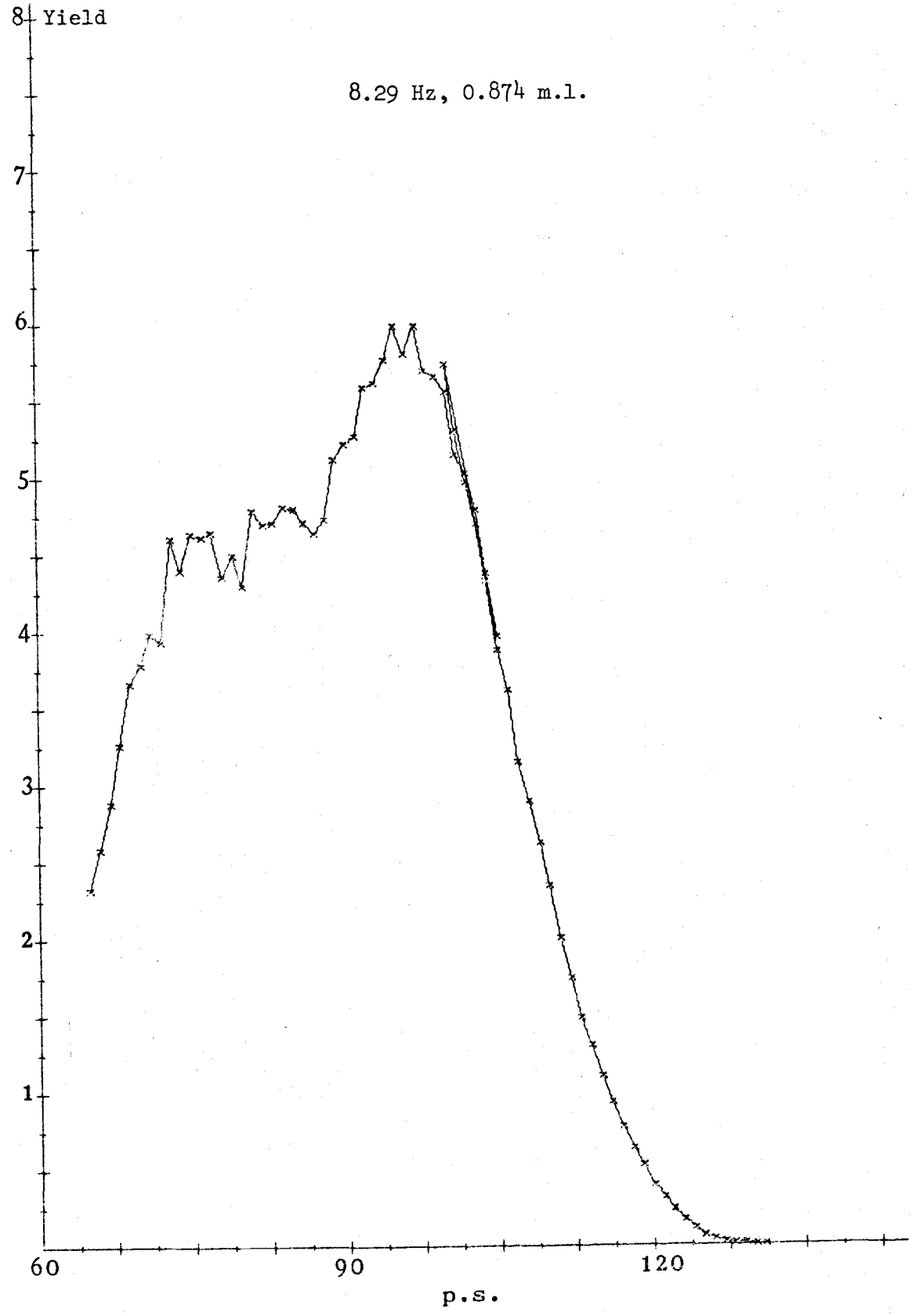
Yield
8.29 Hz, 0.874 m.l.
8
7
6
5
4
3
2
1
60
90
120
p.s.

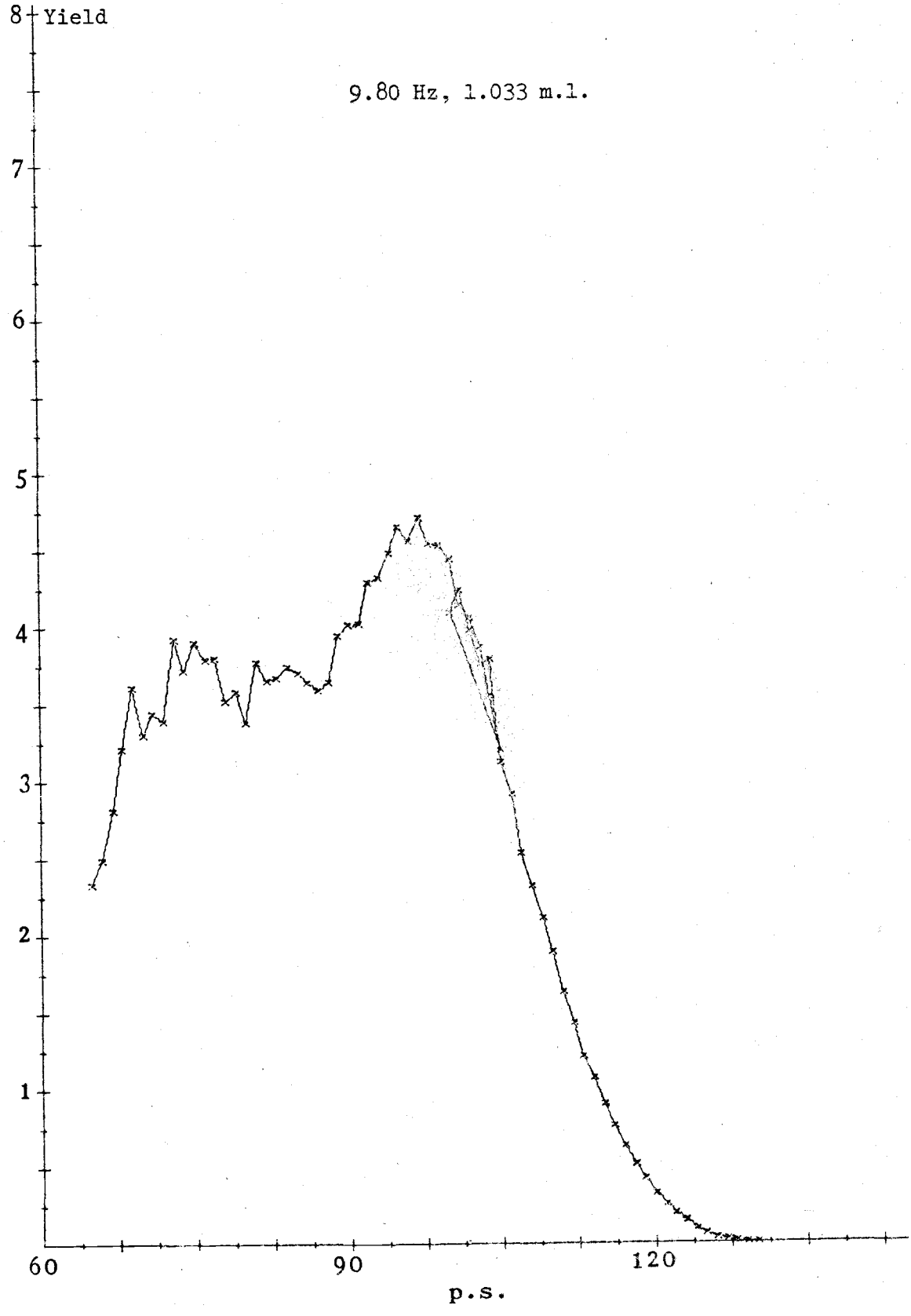
Yield
9.80 Hz, 1.033 m.l.
8
7
6
5
4
3
2
1
60
90
120
p.s.

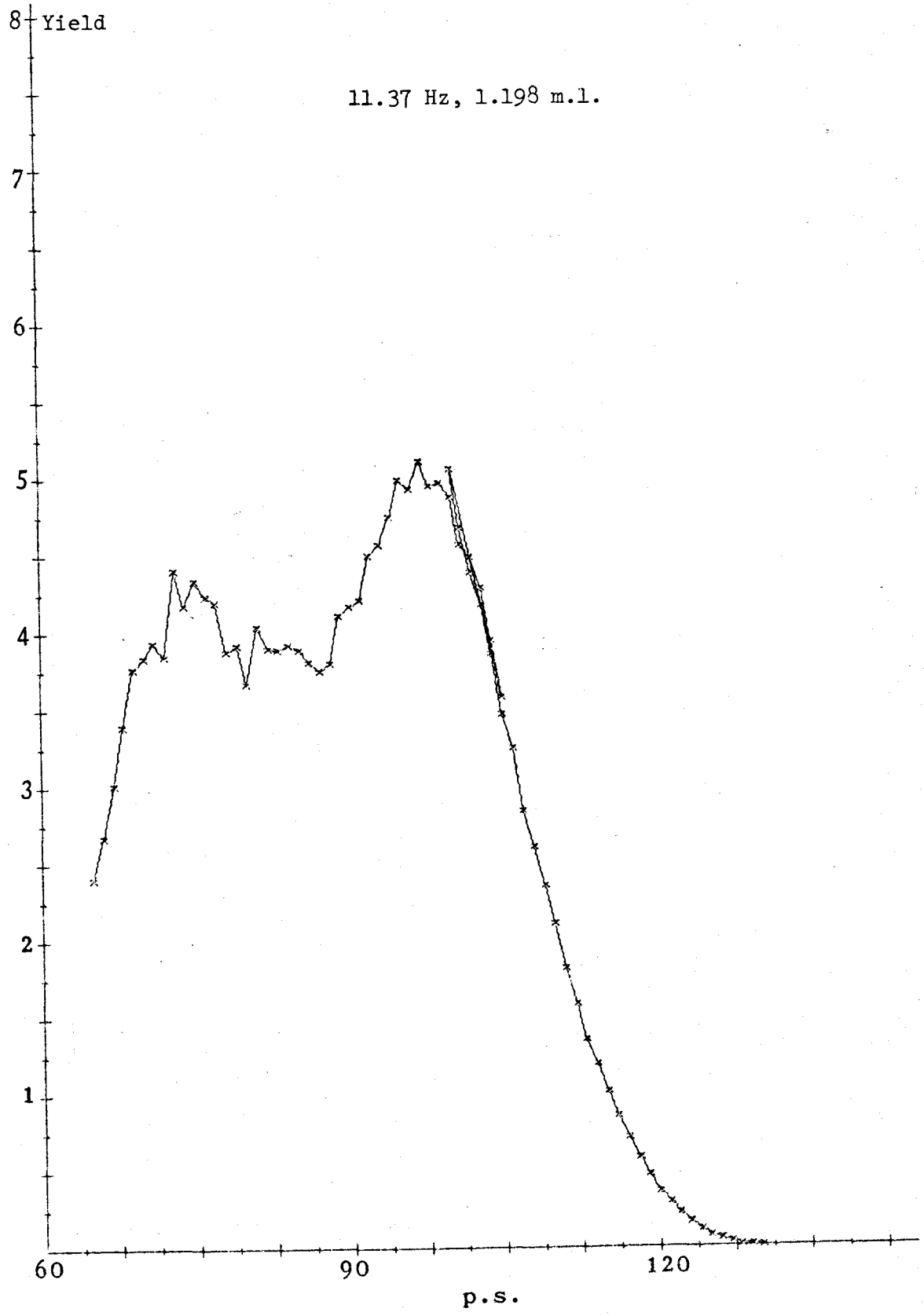
Yield
11.37 Hz, 1.198 m.l.
8
7
6
5
4
3
2
1
60
90
120
p.s.

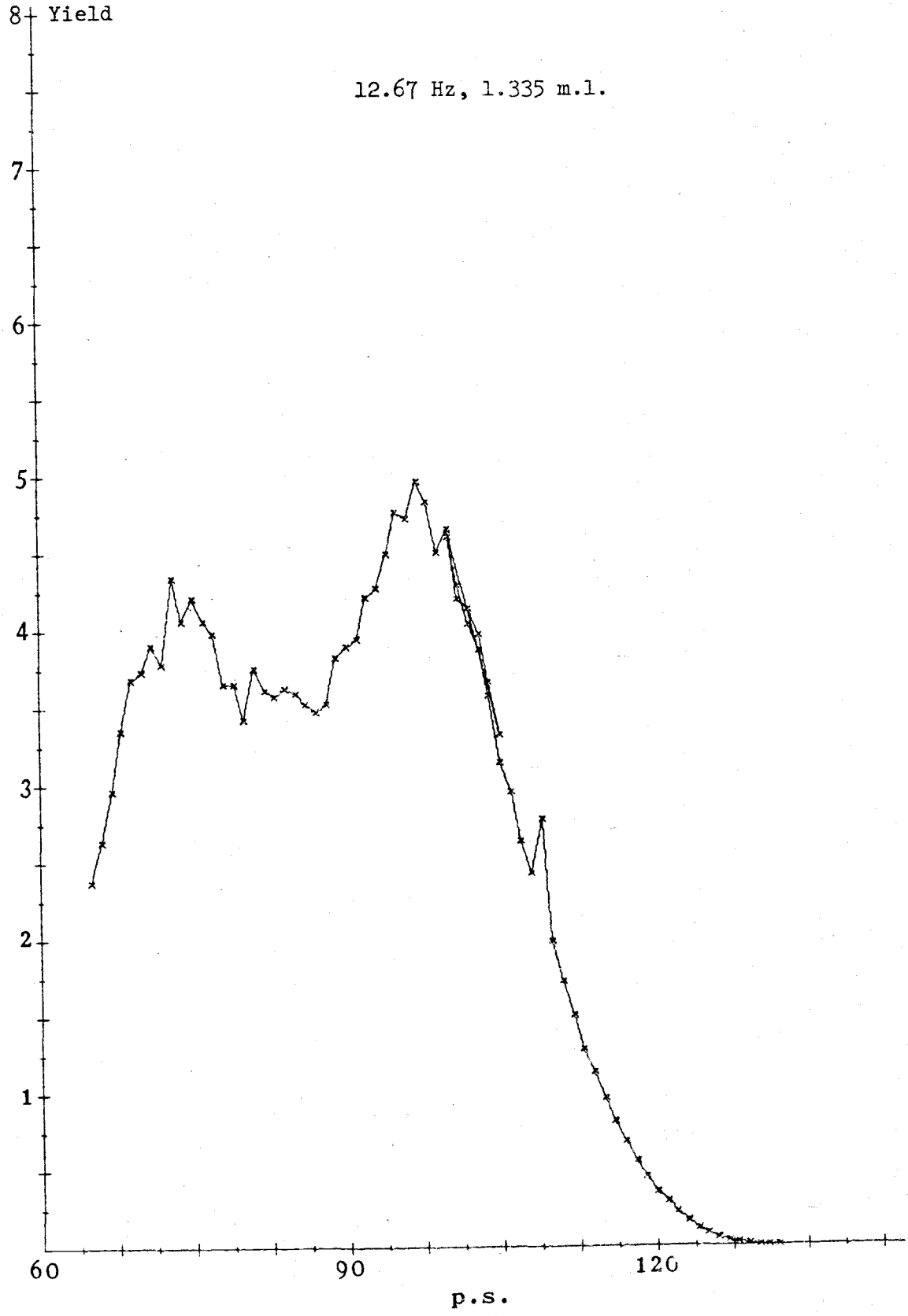
Yield
12.67 Hz, 1.335 m.l.
8
7
6
5
4
3
2
1
60
90
120
p.s.

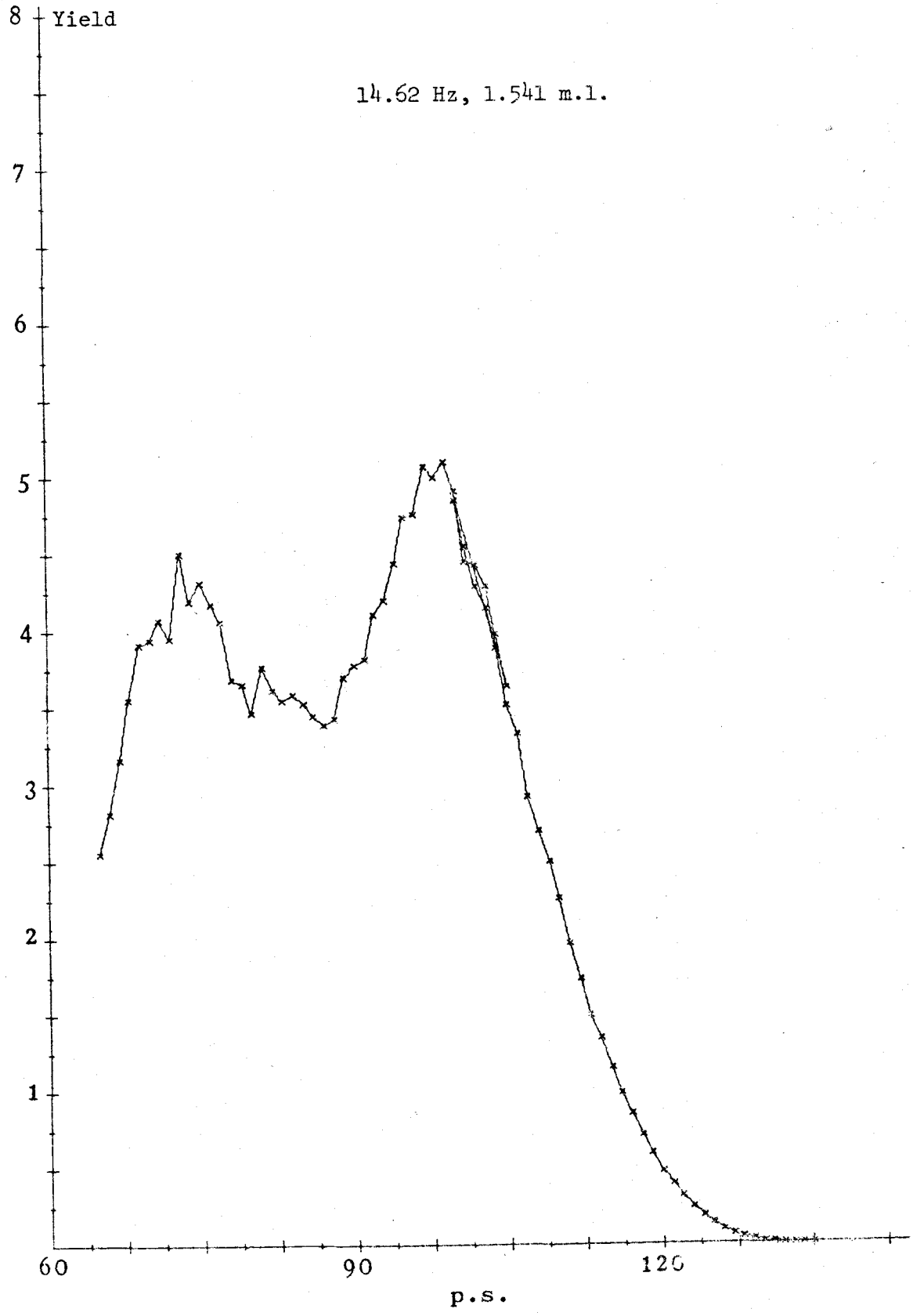
Yield
14.62 Hz, 1.541 m.l.
8
7
6
5
4
3
2
1
60
90
120
p.s.

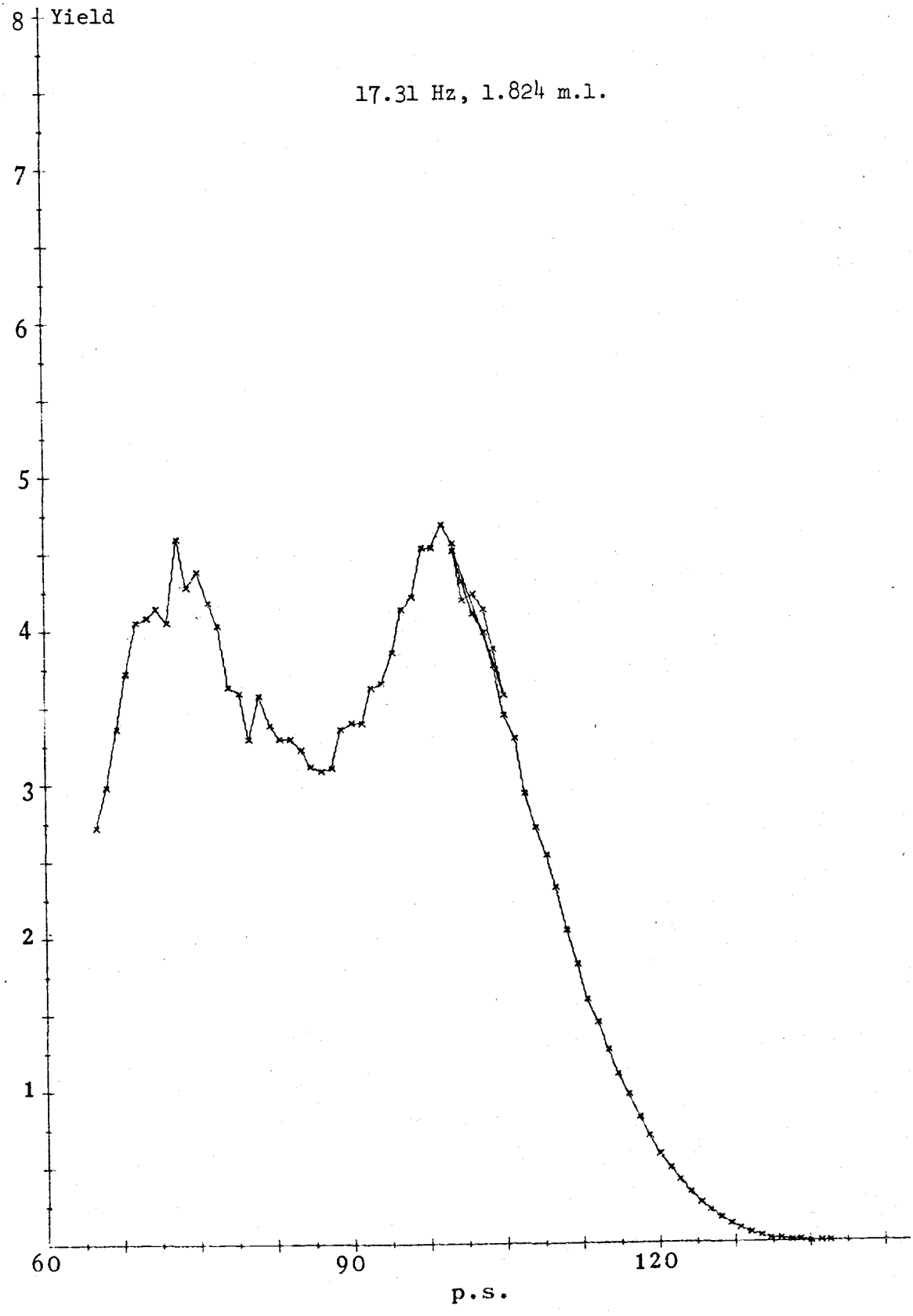
Yield
17.31 Hz, 1.824 m.l.
8
7
6
5
4
3
2
1
60
90
120
p.s.

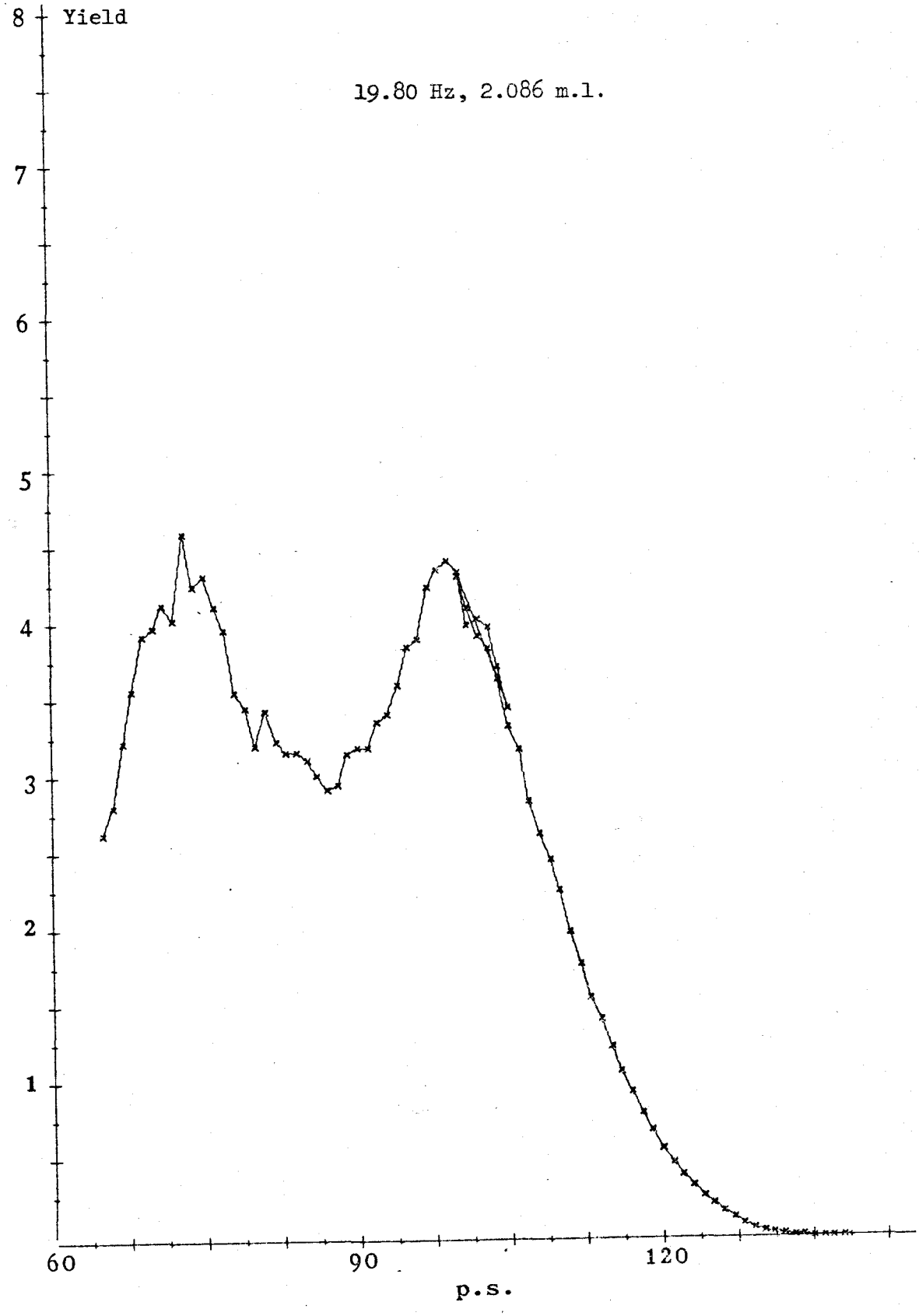
Yield
19.80 Hz, 2.086 m.l.
8
7
6
5
4
3
2
1
60
90
120
p.s.

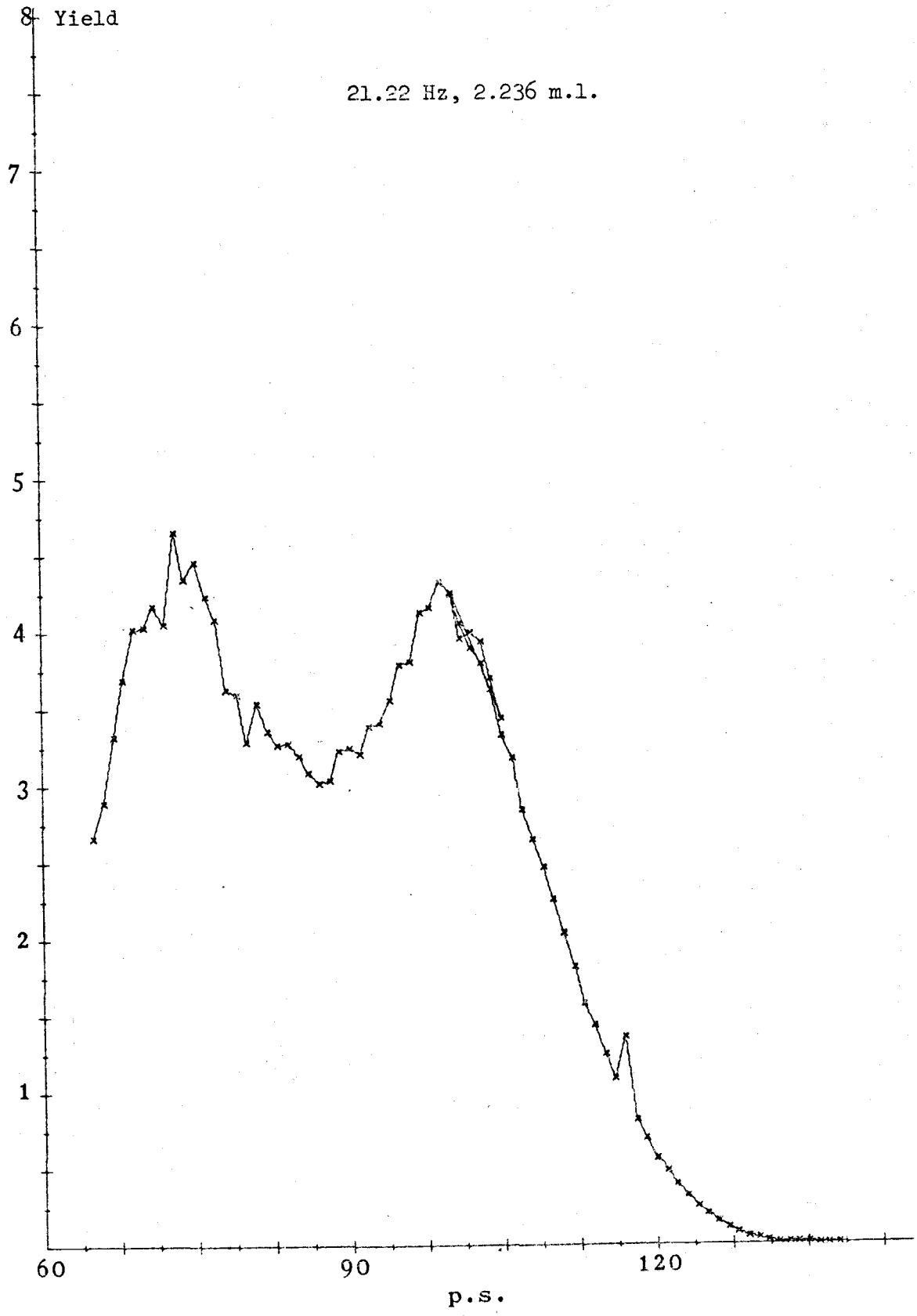
8
Yield
21.22 Hz, 2.236 m.l.
7
6
5
4
3
2
1
60
90
120
p.s.

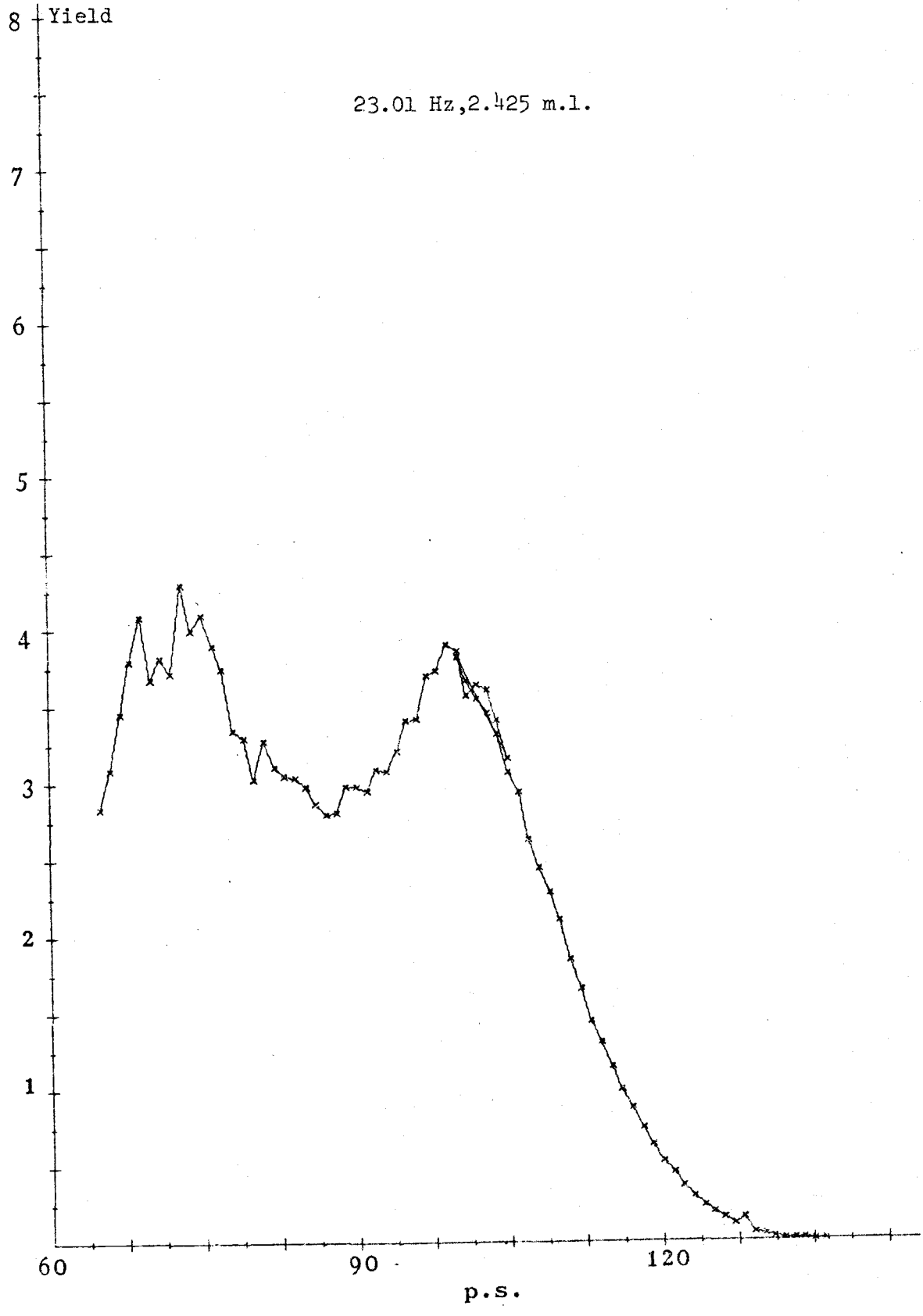
Yield
23.01 Hz,2.425 m.l.
8
7
6
5
4
3
2
1
60
90
120
p.s.

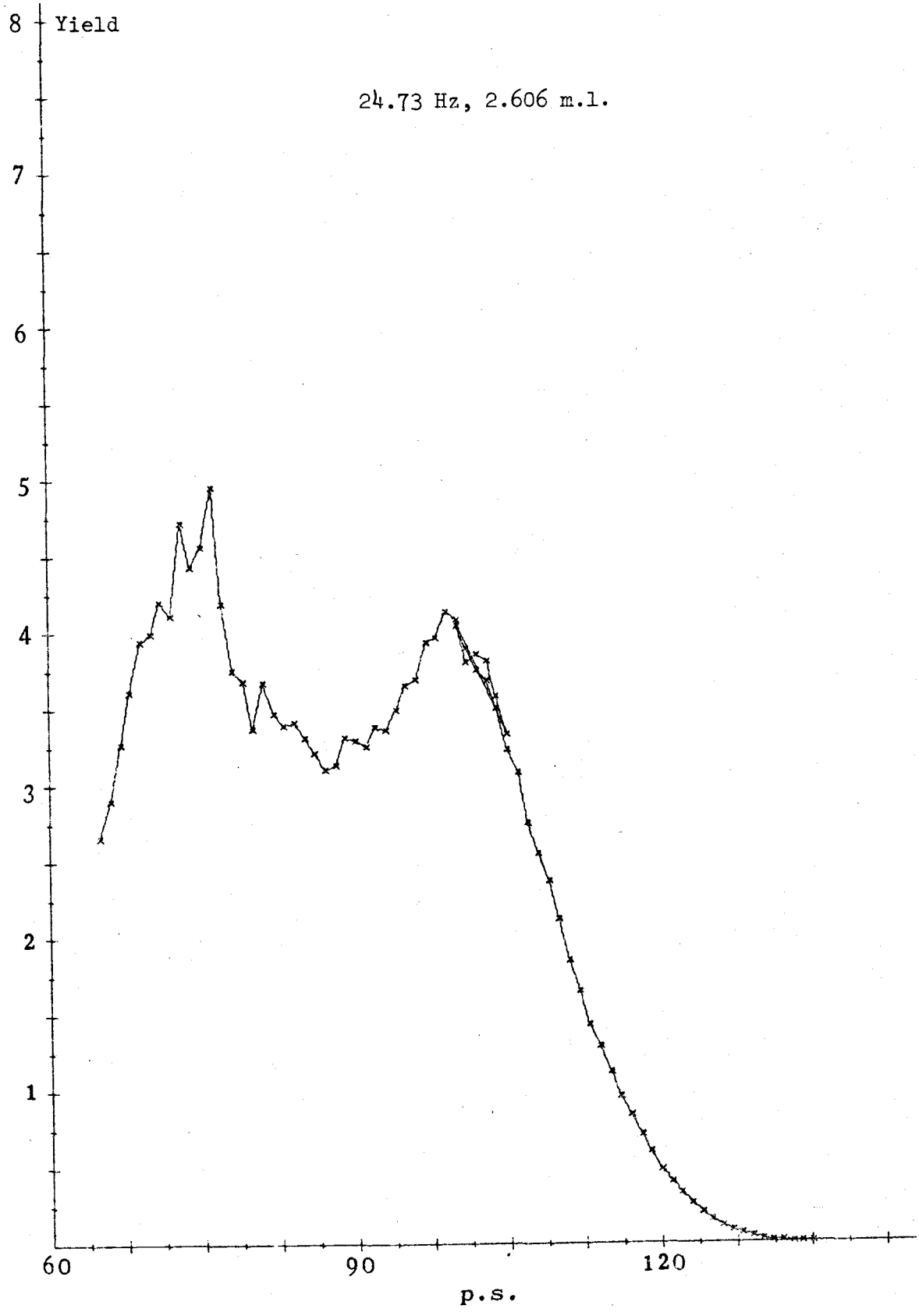
Yield
24.73 Hz, 2.606 m.l.
8
7
6
5
4
3
2
1
60
90
120
p.s.

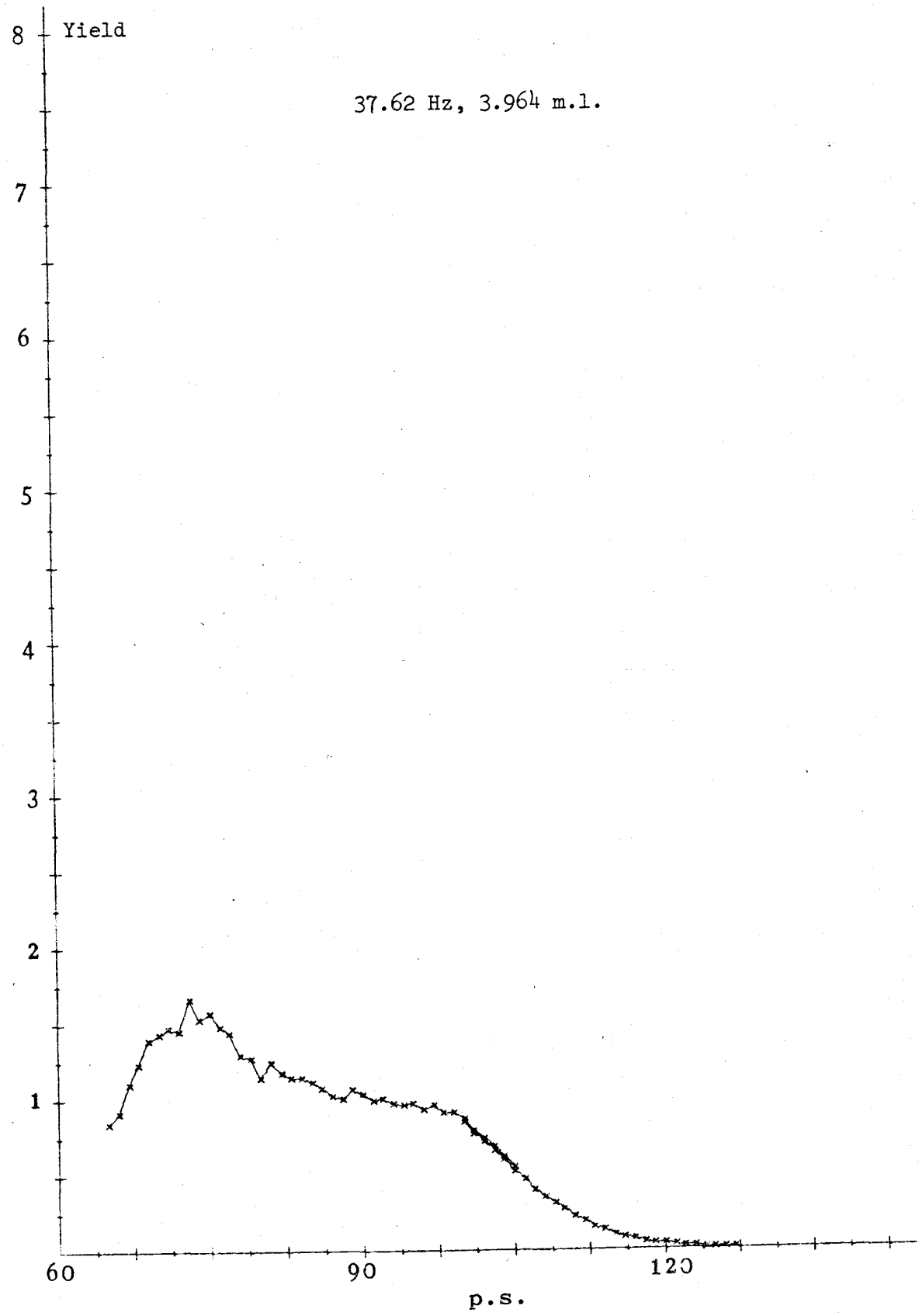
Yield
37.62 Hz, 3.964 m.l.
8
7
6
5
4
3
2
1
60
90
120
p.s.

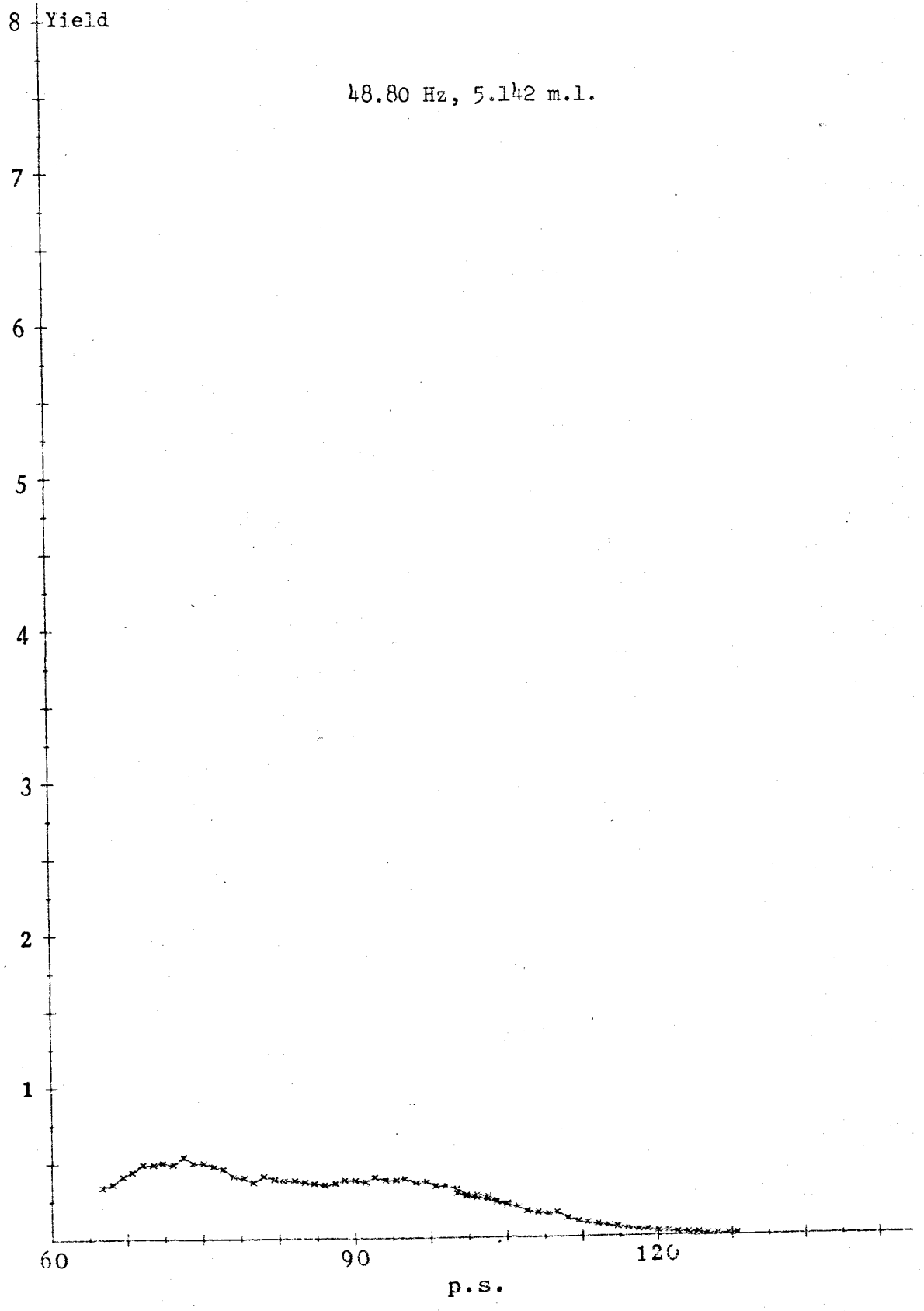
Yield
48.80 Hz, 5.142 m.l.
8
7
6
5
4
3
2
1
60
90
120
p.s.

Table 4. Work functions as determined by the Fowler method, for pure potassium. All the thick samples but one had a double threshold. The thin sample had only a single threshold. The double lines separate data taken on different samples, and the number of days is the time period between the first and last measurement on the same sample.

Work Function		
2.02 (eV)	2.34 (eV)	
2.06	2.33	
2.02	2.33	
2.02	2.32	
2.02	2.33	9 days
2.00	2.32	
2.03	2.31	
2.00	2.31	
2.04	2.30	
2.18	2.34	
2.06	2.36	
2.04	2.36	
2.00	2.35	11 days
2.05	2.35	
2.02	2.35	
2.01	2.32	
1.99	2.40	
--	2.38	
--	2.40	
--	2.39	2 days (thin sample)
--	2.39	
--	2.40	